



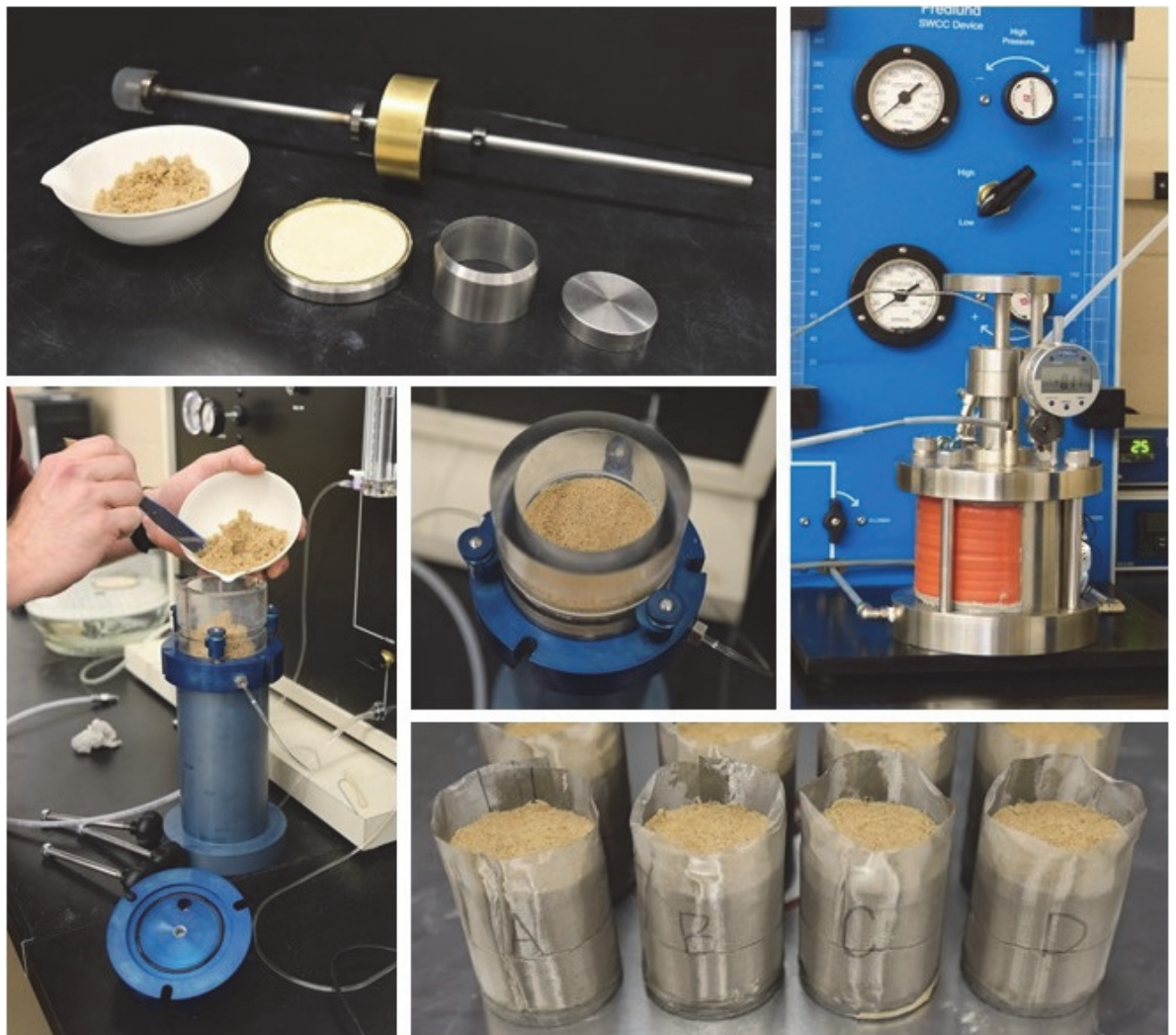
**US Army Corps  
of Engineers®**  
Engineer Research and  
Development Center



## Laboratory Measure of SWCC for a Poorly Graded Fine Sand

Lucas A. Walshire, Oliver-Denzil S. Taylor, and Woodman W. Berry

August 2019



**The U.S. Army Engineer Research and Development Center (ERDC)** solves the nation's toughest engineering and environmental challenges. ERDC develops innovative solutions in civil and military engineering, geospatial sciences, water resources, and environmental sciences for the Army, the Department of Defense, civilian agencies, and our nation's public good. Find out more at [www.erdcl.usace.army.mil](http://www.erdcl.usace.army.mil).

To search for other technical reports published by ERDC, visit the ERDC online library at <http://acwc.sdp.sirsi.net/client/default>.

# **Laboratory Measure of SWCC for a Poorly Graded Fine Sand**

Lucas A. Walshire, Oliver-Denzil S. Taylor, and Woodman W. Berry

*Geotechnical and Structures Laboratory*  
*U.S. Army Engineer Research and Development Center*  
*3909 Halls Ferry Road*  
*Vicksburg, MS 39180-6199*

Final report

Approved for public release; distribution is unlimited.

Prepared for U.S. Army Corps of Engineers  
Washington, DC 20314-1000

Under Project 62784/T40/46, ASA(ALT)

## Abstract

A laboratory testing program was undertaken to investigate the effects of soil fabrics and densities on the Soil Water Characteristic Curve (SWCC) of a poorly graded (SP), fine-grained sand. The program also better developed the capability to assess soils remotely under both discrete and multivariable geotechnical, geological, and environmental conditions. The results initiate both a soils database to define a baseline behavior and a predictive model for changes in soil characteristics (strength) and behavior (volumetric) under varying meteorological conditions.

The laboratory testing program reconstituted the fine-grained sand samples dry of optimum saturation. An energy-based sample preparation method was then used to build samples comparable to *in-situ* soil fabrics. Four preparation reconstitution energies and three saturation levels generated soil fabrics within a band of possible densities limited by the soil's mechanical properties. The Transient Release and Imbibition Method (TRIM), the Fredlund device, and the filter paper method (FPM) were used to develop a statistically representative laboratory SWCC over the range of densities and soil fabrics. Testing results indicate that the Fredlund device and TRIM measure the SWCC independently of preparation energy and saturation, as the mean SWCC and the median, maximum, and minimum curves fall within the same range of values.

**DISCLAIMER:** The contents of this report are not to be used for advertising, publication, or promotional purposes. Citation of trade names does not constitute an official endorsement or approval of the use of such commercial products. All product names and trademarks cited are the property of their respective owners. The findings of this report are not to be construed as an official Department of the Army position unless so designated by other authorized documents.

**DESTROY THIS REPORT WHEN NO LONGER NEEDED. DO NOT RETURN IT TO THE ORIGINATOR.**

# Contents

<b>Abstract.....</b>	<b>ii</b>
<b>Figures and Tables.....</b>	<b>iv</b>
<b>Preface .....</b>	<b>vi</b>
<b>Unit Conversion Factors.....</b>	<b>vii</b>
<b>1 Introduction .....</b>	<b>1</b>
<b>2 Laboratory Testing Protocol.....</b>	<b>12</b>
2.1 Sample preparation.....	12
2.2 Fredlund device .....	14
2.3 TRIM device.....	16
2.4 Filter paper test .....	19
<b>3 Laboratory Testing Results .....</b>	<b>21</b>
3.1 18 percent saturation .....	21
3.2 24 percent saturation.....	27
3.3 30 percent saturation .....	35
<b>4 Discussion.....</b>	<b>40</b>
<b>5 Conclusions .....</b>	<b>55</b>
<b>6 References.....</b>	<b>57</b>
<b>Report Documentation Page</b>	

# Figures and Tables

## Figures

Figure 1. Example SWCC showing how to find the air entry value (AEV) .....	3
Figure 2. Fredlund and Xing and van Genuchten models used to fit laboratory measured data .....	6
Figure 3. Hysteresis of SWCC for a coarse-grained soil.....	7
Figure 4. Example SWCC for clay, silt, and sand .....	8
Figure 5. HCF using van Genuchten and Fredlund and Xing models, coarse-grained soil with a saturated hydraulic conductivity of 0.1 cm/s.....	10
Figure 6. Compaction curve for fine sand, per ASTM D1557 .....	13
Figure 7. Fine-grained sand distribution.....	13
Figure 8. Fredlund device sample preparation.....	15
Figure 9. Sample following saturation loaded into Fredlund device .....	16
Figure 10. TRIM device: (a) disassembled device, (b) stone inserted, and (c) preparing chamber.....	16
Figure 11. TRIM sample construction: (a) loose soil added to chamber, (b) sample compacted, and (c) height measurement.....	17
Figure 12. Assembled TRIM chamber and sample saturating .....	18
Figure 13. PVC filter paper sample holders .....	20
Figure 14. Screen filter paper sample containers.....	20
Figure 15. Sand samples prepared at 18 percent saturation fitted with the van Genuchten model.....	23
Figure 16. Sand samples prepared at 18 percent saturation fitted with the Fredlund and Xing model.....	24
Figure 17. Maximum, minimum, mean, and median SWCC data for samples prepared at a saturation of 18 percent, van Genuchten model.....	26
Figure 18. Maximum, minimum, mean, and median SWCC data for samples prepared at a saturation of 18 percent, Fredlund and Xing model.....	27
Figure 19. Sand samples prepared at 24 percent saturation fitted with the van Genuchten model.....	29
Figure 20. Sand samples prepared at 24 percent saturation fitted with the Fredlund and Xing model.....	30
Figure 21. Maximum, minimum, mean, and median SWCC data for samples prepared at a saturation of 24 percent, van Genuchten model.....	32
Figure 22. Maximum, minimum, mean, and median SWCC data for samples prepared at a saturation of 24 percent, Fredlund and Xing model.....	33
Figure 23. Results of FPM compared to Fredlund and TRIM device mean, maximum, and minimum data.....	34
Figure 24. Sand samples prepared at 30 percent saturation fitted with the van Genuchten model.....	36

Figure 25. Sand samples prepared at 24 percent saturation fitted with the Fredlund and Xing model.....	37
Figure 26. Maximum, minimum, mean, and median SWCC data for samples prepared at a saturation of 30 percent, van Genuchten model.....	38
Figure 27. Maximum, minimum, mean, and median SWCC data for samples prepared at a saturation of 30 percent, Fredlund and Xing model.....	39
Figure 28 Mean SWCC's for 18, 24 and 30 percent saturation levels. ....	41
Figure 29 Variance across preparation energies for samples prepared at 18 percent saturation level .....	42
Figure 30 Variance across preparation energies for samples prepared at 24 percent saturation level .....	43
Figure 31 Variance across preparation energies for samples prepared at 30 percent saturation level .....	44
Figure 32. Maximum, mean, and minimum SWCC values for poorly-graded fine sand fitted with van Genuchten model .....	46
Figure 33. Maximum, mean, and minimum SWCC values for poorly-graded fine sand fitted with Fredlund and Xing model .....	47
Figure 34. UNSODA fine-grained data set fitted with van Genuchten model.....	49
Figure 35. UNSODA fine-grained data set fitted with Fredlund and Xing model.....	49
Figure 36. Grain-size distribution of fine group samples.....	50
Figure 37. UNSODA coarse-grained data set fitted with van Genuchten model .....	51
Figure 38. UNSODA coarse-grained data set fitted with Fredlund and Xing model.....	52
Figure 39. Prediction methods plotted with the minimum, mean, and maximum values .....	54

## Tables

Table 1. Soil properties for 18 percent saturation .....	22
Table 2. SWCC model data for sand samples prepared at 18 percent saturation.....	25
Table 3. Soil properties for 24 percent saturation .....	28
Table 4. SWCC model data for sand samples prepared at 24 percent saturation .....	31
Table 5. Model parameters for the FPM results.....	33
Table 6. 30 percent saturation soil properties .....	35
Table 7. SWCC model data for sand samples prepared at 30 percent saturation .....	37
Table 8. Variation in soil density state for the reconstituted specimens. ....	40
Table 9. Fitting parameters for maximum, mean, and minimum SWCCs.....	45
Table 10. Soils data for samples selected from UNSODA .....	48
Table 11. Fitting parameters for SWCC prediction methods.....	53

## Preface

This project was funded by Assistant Secretary of the Army (Acquisition, Logistics, and Technology [ASA(ALT)]) under 62784/T40/46.

The work was performed by the Structural Engineering Branch (GSS) and Geotechnical Engineering and Geoscience Branch (GSG) of the Geosciences and Structures Division (GS), U.S. Army Engineer Research and Development Center, Geotechnical and Structures Laboratory (ERDC-GSL). At the time of publication, Ms. Mariely Mejias-Santiago was Chief, CEERD-GSS; Mr. Christopher Price was Chief, CEERD-GSG; Mr. James Davis was Chief, CEERD-GS; and Ms. Pamela Kinnebrew, CEERD-GZT, was the Technical Director for Military Engineering. The Deputy Director of ERDC-GSL was Mr. Charles W. Ertle II, and the Director was Mr. Bartley P. Durst.

COL Ivan P. Beckman was the Commander of ERDC, and Dr. David W. Pittman was the Director.

## Unit Conversion Factors

English - Multiply	By	To Obtain - Metric
cubic feet	0.02831685	cubic meters
cubic inches	1.6387064 E-05	cubic meters
cubic yards	0.7645549	cubic meters
feet	0.3048	meters
pounds (force) per foot	14.59390	newtons per meter
pounds (force) per inch	175.1268	newtons per meter
pounds (mass)	0.45359237	kilograms
pounds (mass) per cubic foot	16.01846	kilograms per cubic meter
pounds (mass) per cubic inch	2.757990 E+04	kilograms per cubic meter
yards	0.9144	meters

# 1 Introduction

Historically, geotechnical design and assessment have been concerned with saturated soils; this works well for design because it is a conservative approach. A saturated soil, when compared with an unsaturated soil, has a higher hydraulic conductivity and a lower shear strength. An unsaturated soil has both air and water in the void space between soil grains. As a soil dries, the water content decreases and air content increases. In an unsaturated state, the flow of water is hindered by pockets of air, decreasing the ability for water to move through the void spaces and thereby decreasing the hydraulic conductivity. The decreased water content of the unsaturated soil also has the impact of inhibiting shear strains and increasing the soil's shear strength. A unique relationship exists between the water content of the soil fabric and the pore water pressure. This relationship is defined by the soil-water characteristic curve (SWCC). Through the description of these processes, it is apparent that the SWCC is central in defining an unsaturated soil's behavior. Unsaturated soils make up a majority of the near-surface soils located above the water table.

The aim of this laboratory investigation is to increase the capability to assess soils remotely under discrete and multivariable conditions by defining the range of SWCC per soil type. The results presented herein are for a poorly graded, fine-grained sand, but testing is underway to define this range for other soil types. Results of these investigations will follow in additional reports. The following list describes the ultimate objectives of this research:

- Generate a database of soils for which proxy soils can be constructed to represent the characteristics of predominate Unified Soil Classification System (USCS; ASTM 1998) soils.
- Investigate the influence of the geological depositional environment on the soil structure and the behavior of the soils represented in the constructed database.
- Develop statistical bounds for soils represented in the soils database.
- Develop a method for incorporating the soils database into existing world soils maps.

The current laboratory investigation was initiated by measuring the SWCC for a fine-grained sand. According to the USCS, the sand used in this investigation classifies as a poorly graded sand (SP), and the range of particle sizes falls within the fine-grained band. The SWCC was measured using two laboratory methods: axis translation and filter paper. The Fredlund device and the Transient Release and Imbibition Method (TRIM) both use the axis translation. The filter paper method (FPM) employs a correlation between the water content of filter paper and the negative pore pressure in the soil. The samples were prepared by using a method that is highly repeatable to reduce laboratory uncertainty by controlling the three principal components of sample reconstitution: mass, water, and applied energy. The method includes using multiple energy levels in an attempt to understand the impact of sample preparation on the results of SWCC testing.

Additional SWCCs of cohesionless and low plasticity sandy soils (SP-SM, SW-SM, and SM) were integrated into the presented findings. These SWCCs were found in the Unsaturated Soil Data (UNSODA) Hydraulic Database (Nemes et al. 1999) and were used to assess the validity of the results of the current laboratory investigation.

Considering near-surface soils, defined as soils within one meter of the ground surface that impact mobility and maneuverability, it is imperative to consider how fluid stored in the soil migrates into and migrates out of the soil and how the soil behaves as a result (e.g., shear strength, volumetric behavior). Moisture storage and moisture movement in unsaturated soils vary temporally and spatially as a result of the storage capacity of the soil and time-dependent changes such as rainfall or other surface saturation processes (Lu and Likos 2004). With regard to storage and fluid flow, the governing equation is obtained from mass conservation; it was derived by Richards (1931) and is presented in Equation 1 from Lu and Likos (2004).

$$\frac{\partial}{\partial x} \left[ k_x(h_m) \frac{\partial h_m}{\partial x} \right] + \frac{\partial}{\partial y} \left[ k_y(h_m) \frac{\partial h_m}{\partial y} \right] + \frac{\partial}{\partial z} \left[ k_z(h_m) \left( \frac{\partial h_m}{\partial z} + 1 \right) \right] = \frac{\partial \theta}{\partial h_m} \frac{\partial h_m}{\partial t} \quad (1)$$

Where  $k$  is the directional component of the soil's hydraulic conductivity (in the  $x$ ,  $y$ , or  $z$  direction),  $h_m$  is the matric suction head, and  $\theta$  is the volumetric water content. The term  $\frac{\partial \theta}{\partial h_m}$  is the slope of the SWCC; thus,

Eq.1 shows that the total flux into a soil system is equal to the soil storage and the total flux out.

The SWCC is the relationship between soil moisture content and pore pressure with soil suction defined as negative pore water pressure. Total suction consists of two primary components: matric suction and osmotic suction (Fredlund et al. 2012). Matric suction (also known as capillary pressure) is the mathematical difference between the air pressure and water pressure ( $u_a - u_w$ ) in the soil. The air pressure is usually zero gauge, and the water pressure is negative due to surface tension. Osmotic suction is associated with both saturated and unsaturated soils and is related to the salt content in the pore-water. If the salt concentration in the pore fluid changes, there is a corresponding change in the volume and the shear strength of the soil (Fredlund and Rahardjo 1993). For the purpose of this report, osmotic suction will not be considered because it was deemed to play a minor role compared to the matric suction. Thus, the SWCC defines how the water content changes with increasing matric suction (see Figure 1 for an example SWCC of a sandy soil).

Figure 1. Example SWCC showing how to find the air entry value (AEV).

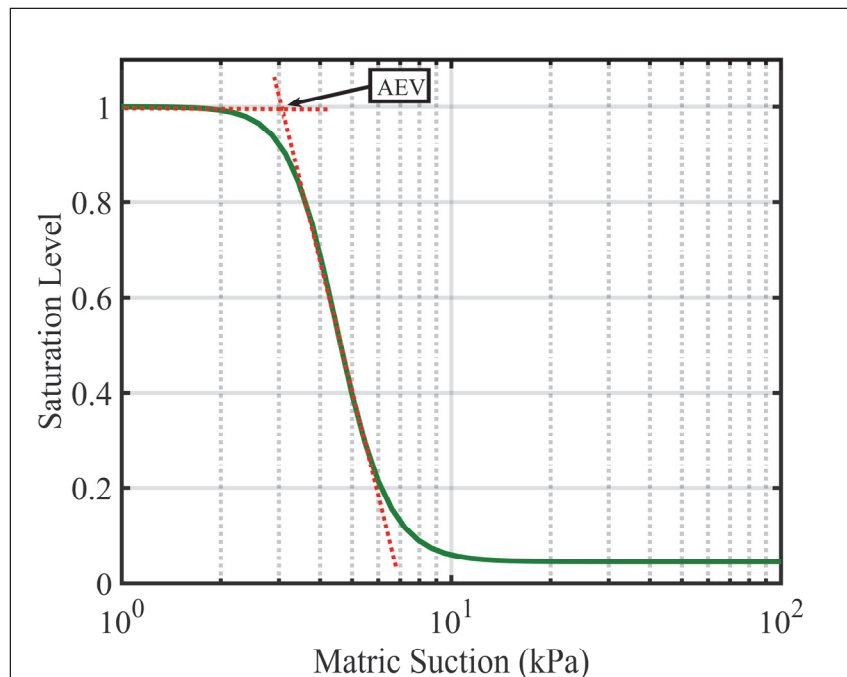


Figure 1 shows the degree of saturation on the vertical scale and the matric suction on the horizontal scale with a logarithmic horizontal scale. Although the degree of saturation is shown, this axis may be displayed in

terms of gravimetric or volumetric water content. Coarse-grained soils exhibit a reverse S-shaped SWCC where the region between the two breaks in slope represents the largest desaturation of the pore space between soil grains. The point at which the largest pore spaces begin to desaturate is termed the air entry value (AEV) and is depicted in Figure 1. The AEV is determined by locating the inflection point (point of maximum curvature of SWCC) and drawing a line tangent to this point. A horizontal line is drawn at 100 percent saturation, and where this line intersects the tangent is the AEV (in units of pressure). The residual suction is defined by the point at which the pore water is held from a capillary force to being dominated by adsorption forces (Vanapalli et al. 1998).

One of the laboratory methods in this investigation used the axis translation technique. At a negative or tensile pressure of approximately -1 atm, water will cavitate. Cavitation is the formation of gas bubbles in a liquid as a result of a decrease in pressure that falls at or below the vapor pressure of the liquid (Trevena 1984). Large negative pore water pressures have been measured in pore water and yet cavitation has not been observed. An explanation for this was presented in Olson and Langfelder (1965): they stated that water does not cavitate in the pore space of soils due to the adsorptive forces and force distribution within pore water. In the laboratory, water cavitation has been a major obstacle to measuring the SWCC. The axis translation technique is used to overcome this obstacle. The axis translation technique utilizes the definition of matric suction, Equation 2.

$$\psi = u_a - u_w \quad (2)$$

where  $\psi$  is matric suction,  $u_a$  is air pressure, and  $u_w$  is pore-water pressure. Where the water pressure is maintained at a low value and air pressure is increased, by using this technique, large values of matric suction can be attained without cavitation of the pore water. This is the central tenant of the axis-translation technique of measuring matric suctions greater than 1 atm. The axis translation technique allows for the measurement of the SWCC directly up to 1500 kPa. This limiting value is due to the AEV of the ceramic stones used in laboratory testing.

Once a discrete set of measurements is made, a mathematical model can be fitted to the data to make a continuous SWCC. Two models that are commonly used are the van Genuchten (1980) and the Fredlund and Xing

(1994) models. The van Genuchten model is based on Mualem's model (van Genuchten 1980):

$$\theta = \theta_r + \frac{(\theta_s - \theta_r)}{\left[1 + (\alpha\psi)^n\right]^m} \quad (3)$$

where,  $\theta$ ,  $\theta_r$ , and  $\theta_s$  are the volumetric, residual volumetric, and saturated volumetric water contents, respectively. The values  $\alpha$  (in units of 1/pressure),  $n$ , and  $m$  are fitting parameters; and  $\psi$  is the matric suction. The fitting parameter  $m$  was assumed to be  $1-1/n$ . Another model was proposed by Fredlund and Xing (1994):

$$\theta = C(\psi) \frac{\theta_s}{\left\{ \ln \left[ e + \left( \frac{\psi}{a} \right)^n \right] \right\}^m} \quad (4)$$

where  $\theta_s$  is the saturated volumetric water content,  $\theta$  is the volumetric water content,  $e$  is the natural number (2.71828..), and  $\psi$  is matric suction. The coefficients  $a$  (in units of pressure),  $n$ , and  $m$  are fitting parameters. The coefficient  $C(\psi)$  is a correction factor that forces the model to zero at a matric suction of 1e6 kPa and is defined as:

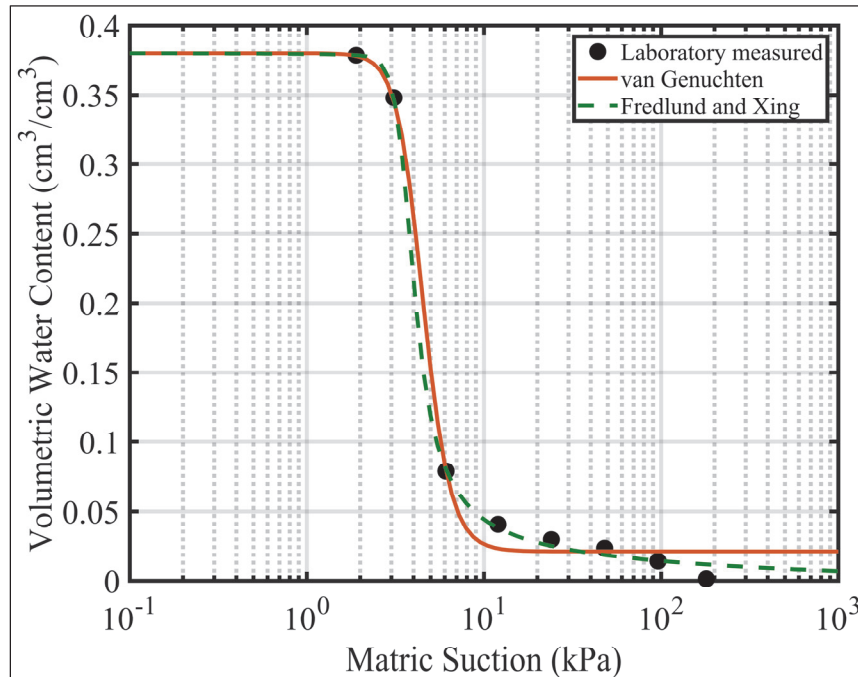
$$C(\psi) = 1 - \frac{\ln \left( 1 + \frac{\psi}{\psi_r} \right)}{\ln \left( 1 + \frac{1e6}{\psi_r} \right)} \quad (5)$$

where  $\psi$  is matric suction and  $\psi_r$  is the residual suction. Fredlund and Xing (1994) suggested that  $\psi_r$  values of between 1500 and 3000 kPa would be generally acceptable approximations.

Both models are continuous and fit the data well with the major difference being that after the residual point, the Fredlund and Xing model reduces to zero at 1e6 kPa while the van Genuchten model maintains a constant water content value. Figure 2 shows the two models fitted to the fine-grained sand laboratory data. Figure 2 shows little variation between the models near the AEV; but at the residual point, the two models diverge slightly. The difference may be minor when the residual water content

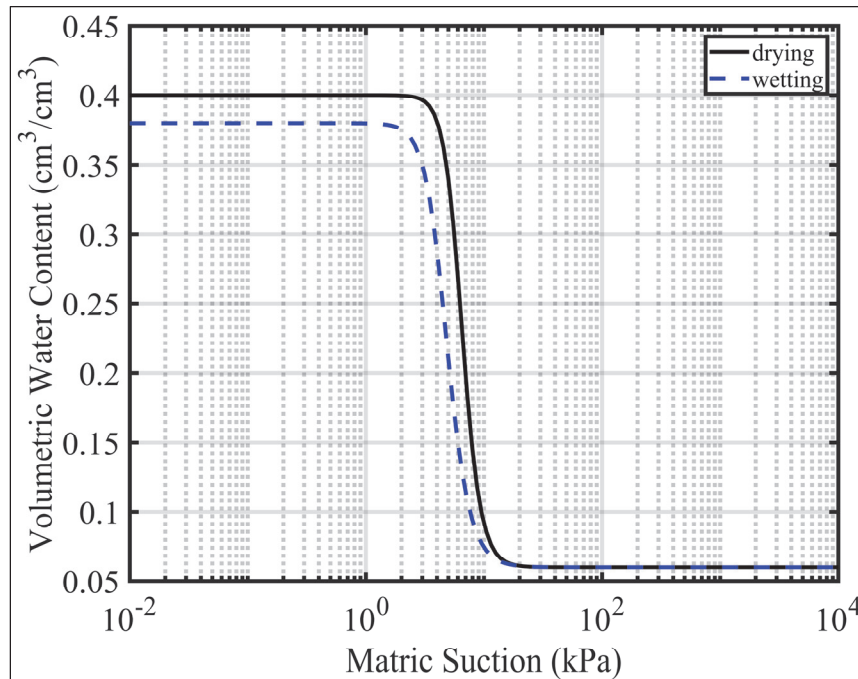
values are small ( $<0.04$ ) but at larger residual water content values, there may be a significant difference.

Figure 2. Fredlund and Xing and van Genuchten models used to fit laboratory measured data.



Soil desaturation and saturation is a path-dependent process, and the SWCC exhibits hysteresis during wetting and drying processes. Figure 3 shows the difference between the wetting and the drying SWCCs. One observation is that the curves do not share the same saturated water content, and the AEV and water entry value are not the same. This is due to occluded air's being trapped in the pore space during wetting of the soil. Lu et al. (2014) performed an experiment over positive and negative matric suctions to determine the conditions under which this loop would close. They found that as much as -10 kPa of matric suction was needed to fully saturate a soil from a wetting to a drying SWCC for sandy to clayey soils.

Figure 3. Hysteresis of SWCC for a coarse-grained soil.



Likos et al. (2013) performed an extensive study of a wide range of soil types to define the uncertainty of the hysteretic behavior of the SWCC. As a result of this study, they were able to make recommendations with regard to transforming drying curve parameters to wetting curve parameters with regard to the van Genuchten model. They found the following relationships were appropriate:

$$\theta_s^w = 0.85\theta_s^d \quad (6)$$

$$\alpha^w = 2.2\alpha^d \quad (7)$$

$$n^w = n^d \quad (8)$$

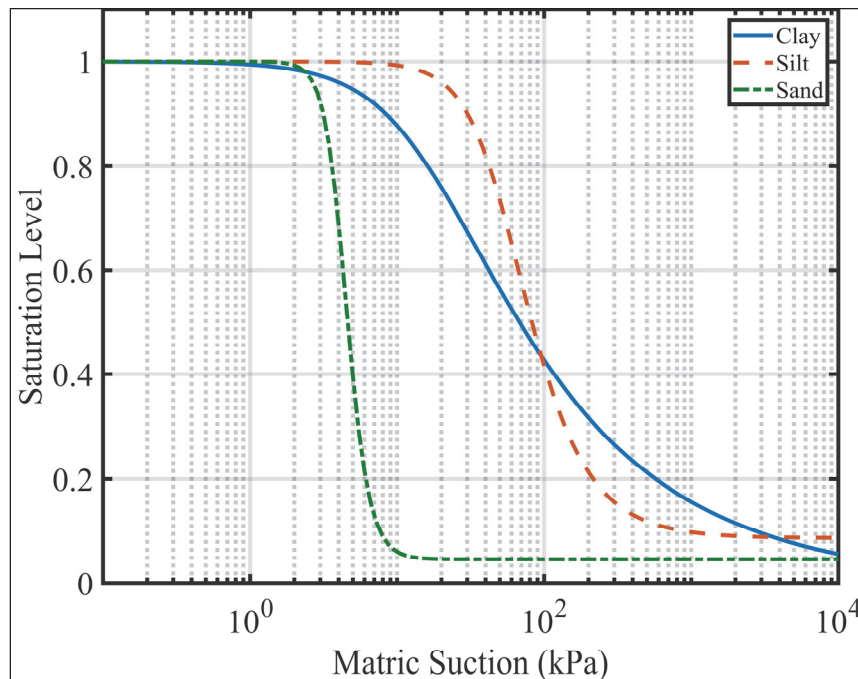
where the superscripts in Equations 7-8,  $w$  and  $d$ , denote wetting and drying and the other parameters are defined according to Equation 3. When using Equations 6 and 7, the residual water content for both the wetting and drying states will remain equal.

With regard to the fitting parameters for the two models, each parameter controls a different portion of the shape of the SWCC. Leong and Rahardjo (1997) showed that the terms  $a$  from Fredlund and Xing's model and  $\alpha$  from van Genuchten's model effectively control where the AEV will occur.

Increasing or decreasing these values will translate the SWCC horizontally. The parameter  $n$  from both models controls the steepness of the desaturation portion of the SWCC, and the parameter  $m$  from both models controls the second break in the SWCC.

Figure 4 shows some typical SWCCs for three soil types: sand, silt, and clay. The curves use the van Genuchten model; and  $\alpha$  values are 0.06, 0.02, and 0.23 1/kPa for clay, silt, and sand, respectively. A trend can be noted with regard to  $\alpha$  values that the SWCCs are translated to the right (increasing suction) with decreasing  $\alpha$  values. The  $m$  values were dependent on  $n$  ( $m=1-1/n$ ); but the  $n$  values for these curves are 1.45, 2.5, and 6.05 for clay, silt, and sand respectively. With a lower  $n$  value, the slope of the SWCC along the main desorption path will be shallower; and at larger matric suction values, the soil will retain more moisture.

Figure 4. Example SWCC for clay, silt, and sand.



Lu and Likos (2004) showed an interpretation of the conceptual model by McQueen and Miller (1974) for regions of the SWCC. This conceptual model showed that at matric suctions greater than the AEV and smaller than the residual matric suction value, the pore water was held in the pore space by capillary forces. At matric suction greater than the residual value, an adsorbed film region and a tightly adsorbed region occur. In the adsorbed film region, water is retained in thin films on the particle

surfaces (Lu and Likos 2004) and, in the tightly adsorbed region, water is retained by molecular bonding.

The capillary region in sandy soils will cover a small range of matric suctions; and with increasing matric suction, the soil desorbs rapidly. This can make testing sandy soils difficult. The limitation of fine-grained soils is that the AEV can be large and difficult to measure by using the axis-translation technique. Therefore, the FPM is often used in conjunction with the axis-translation technique to build a full SWCC dataset.

Once a representative SWCC is obtained, the unsaturated hydraulic conductivity function (HCF) can then be obtained with knowledge of the saturated hydraulic conductivity function. Unsaturated hydraulic conductivity is not constant, and the largest magnitude is the saturated hydraulic conductivity. If the van Genuchten model is used, then Equation 9 can be used to define the HCF.

$$k(h_m) = k_{sat} \left\{ \frac{\left\{ 1 - (\alpha h_m)^{n-1} \left[ 1 + (\alpha h_m)^n \right]^{-m} \right\}^2}{\left[ 1 + (\alpha h_m)^n \right]^{m/2}} \right\} \quad (9)$$

where  $\alpha$ ,  $n$ , and  $m$  are the same parameters previously defined for the SWCC. The parameters  $k$  and  $k_{sat}$  are the unsaturated and saturated hydraulic conductivities, respectively. Another approach is that suggested by Fredlund and Xing (1994) and shown in Equation 10.

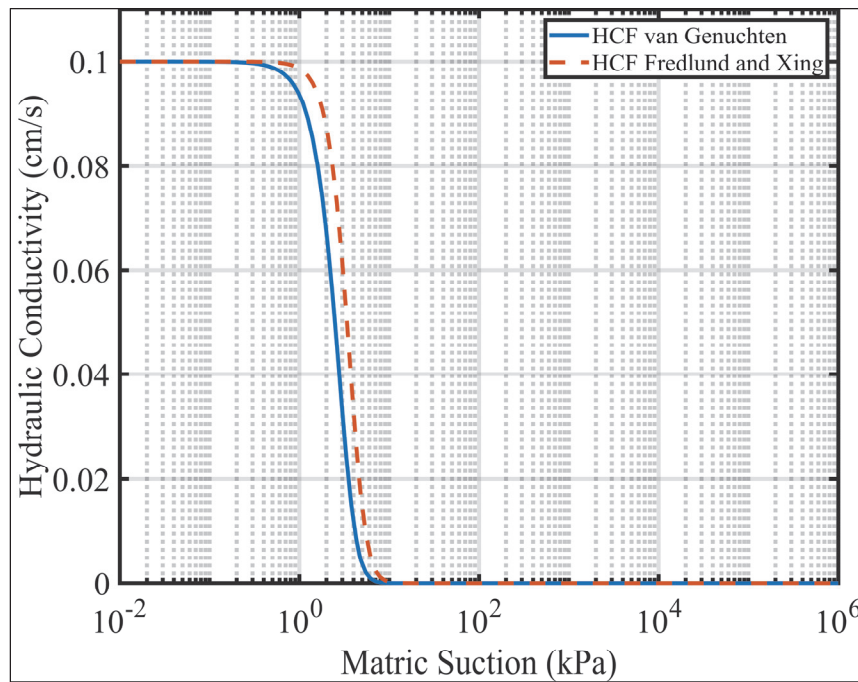
$$k = k_{sat} \frac{\sum_{i=j}^N \frac{\theta(e^y) - \theta(h_m)}{e^{y_i}} \theta'(e^{y_i})}{\sum_{i=1}^N \frac{\theta(e^y) - \theta(h_m)}{e^{y_i}} \theta'(e^{y_i})} \quad (10)$$

where  $\theta$  is the volumetric water content,  $\theta'$  is the first derivative of the model equation,  $e$  is the natural number (2.71828...),  $j$  is the smallest matric suction to be used in the function, and  $i$  is the interval between  $j$  and  $N$ . The parameter  $N$  is the largest matric suction to be used, and  $y$  is a dummy variable.

Figure 5 shows a comparison of the two approaches. There is a slight difference at low suction values. At high suction values the hydraulic

conductivity approaches zero. The Fredlund and Xing method can be used on either model while the van Genuchten approach can be used only with its own SWCC model.

Figure 5. HCF using van Genuchten and Fredlund and Xing models, coarse-grained soil with a saturated hydraulic conductivity of 0.1 cm/s.



There are multiple unsaturated shear strength models available with no widespread consensus on what is appropriate. A method proposed by Lu and Likos (2006) has promise, but further research into its application is needed. Lu and Liko's method involves estimating the unsaturated shear strength function by using the HCF and the SWCC.

Energy application during cohesionless soil sample preparation significantly influences behavior, strength characteristics, and repeatability, resulting in high degrees of epistemic uncertainty within laboratory testing and analyses. Relative density and void ratios have been used to compare materials and specimens in an attempt to address this uncertainty. However, the maximum void ratio of the material is often determined by wet or air pluviation, while the minimum void ratio is determined by vibratory compaction, yet actual sample preparation may use another method. Each method yields different soil fabric and behaviors unrelated to soil mechanics.

The lack of standardized protocols for cohesionless sample preparation can result in numerous confrontational analyses, which are more likely an artifact of sample preparation techniques rather than intrinsic behavior. To accurately compare two materials, consideration must be made to the method by which the sample is made and the normalization method used to account for variability in physical properties between the sample materials. Research by Taylor et al. (2017) developed a standardized protocol for specimen preparation that enables the use of soil strength curves based on expedient field classification testing (e.g., grain size analyses) using a normalization approach to sample preparation that replaces the common relative density method of evaluating the engineering behavior of soils. To prepare consistent, highly repeatable test samples researchers rely on highly controlled compactive energy instead of density and/or void ratio methods. A comprehensive study on the reconstitution of cohesionless samples can be found in Taylor et al. (2017) and Winters et al. (2016).

## 2 Laboratory Testing Protocol

### 2.1 Sample preparation

The sample preparation method used in the Fredlund, TRIM, and FPM tests followed the procedures outlined in Taylor et al. (2017). Using this method, the samples were constructed from a fine sand, compacted by using an energy-based compaction method that ensured a repeatable initial soil fabric (Taylor et al. 2017). For experimental validation, all samples were reconstituted at a remolding saturation of 18 percent, 24 percent, and 30 percent using a range of compaction energies from 200-1000 kJ/m<sup>3</sup> for comparison to field conditions observed by Taylor et al. (2017). To reduce epistemic uncertainty from sample preparation, samples exceeding a 2-percent differential from either targeted saturation or volume were discarded. By controlling the soil mass saturation and compactive energy, sample preparation inconsistencies, as noted by Mulilis et al. (1977), were effectively eliminated and comparable fabric between samples was maintained.

Optimum water content of the fine sand used in this study was 6.94 percent and maximum dry density was 1.78 g/cm<sup>3</sup>. The degree of saturation corresponding to optimum water content was found to be approximately 35 percent. The three remolding saturations chosen for this study were all dry of optimum. Figure 6 shows the compaction curve corresponding to the modified Proctor effort as prescribed in ASTM D1557 (2012).

Figure 6. Compaction curve for fine sand, per ASTM D1557 (2012).

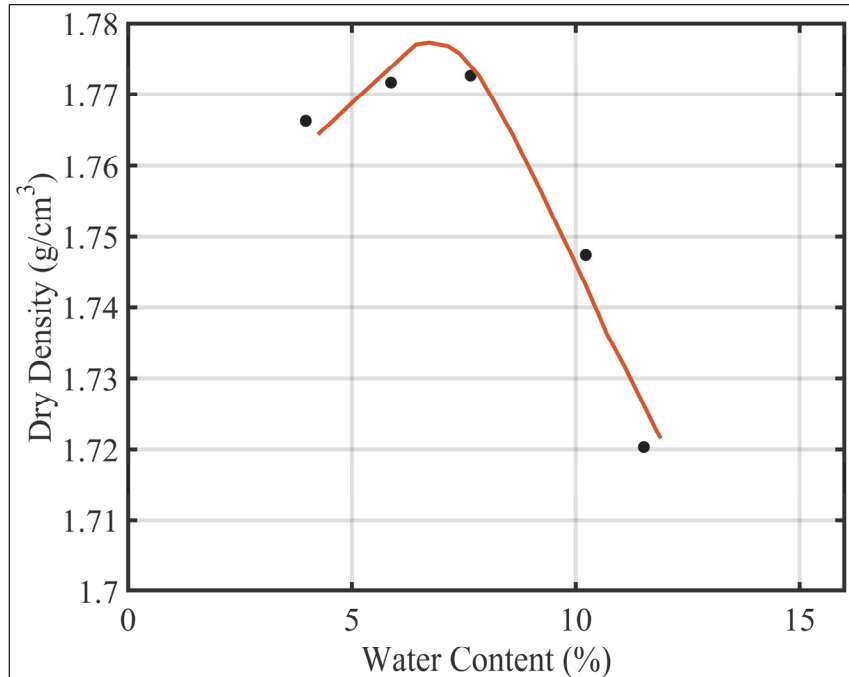
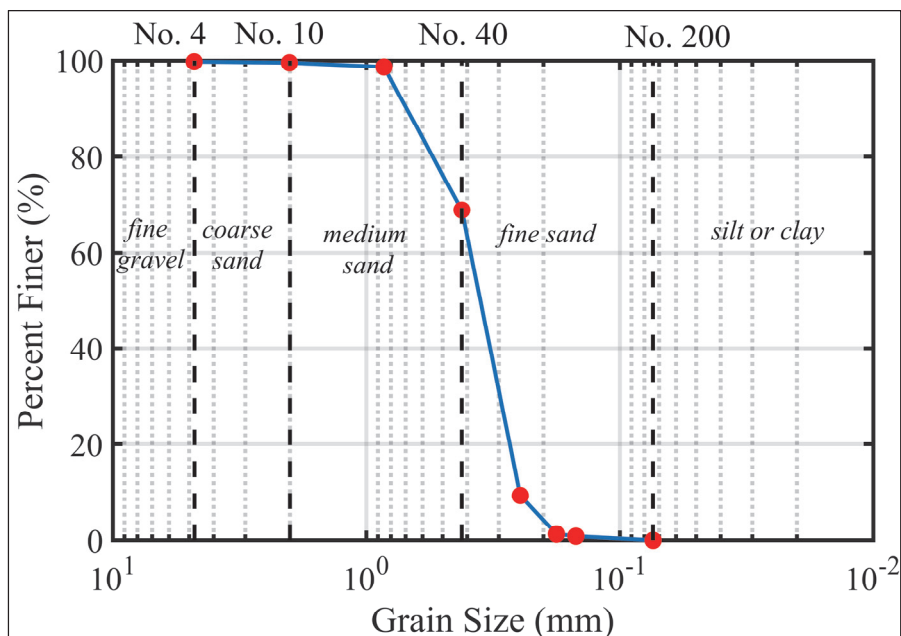


Figure 7 shows the grain-size distribution of the sand used in this investigation. The coefficient of uniformity and curvature were 1.52 and 1.12, respectively, which, according to the USCS (ASTM 1998), classifies as a poorly graded sand. The majority of material lies between the number 40 and 200 sieve sizes, indicating that the material is a fine sand.

Figure 7. Fine-grained sand distribution.

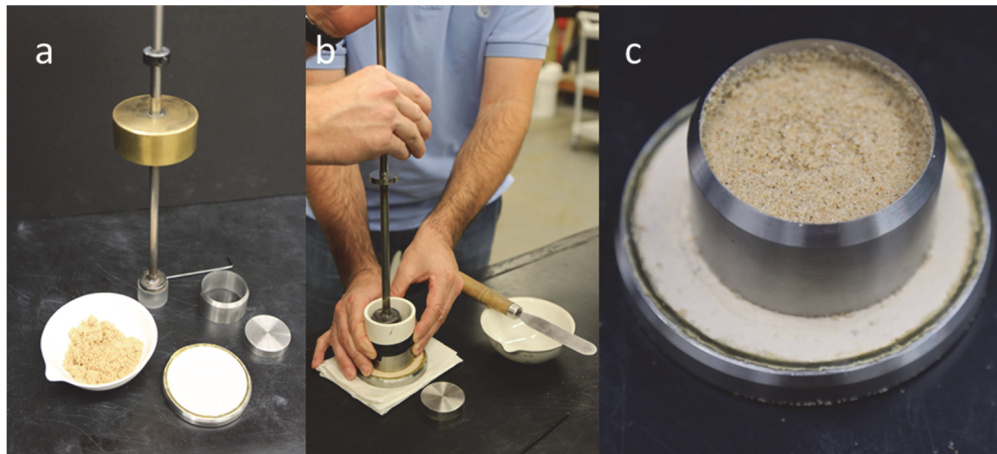


## 2.2 Fredlund device

Samples prepared for the Fredlund device were constructed in a steel cylinder with an inside diameter of 5.06 cm and a height of 3.16 cm. Four samples were prepared by using a different energy for each sample (i.e., 200, 300, 600, or 1000 kJ/m<sup>3</sup>). The samples were compacted in a single lift by using a rammer with an acrylic foot diameter of 3.55 cm. The mass and drop height of the rammer were adjusted depending on the desired energy level. Figure 8a shows the rammer and the material necessary to construct the Fredlund samples. Prior to sample construction, a three-bar-high air entry stone was saturated by placing it into a desiccator with a vacuum pressure of 22 in. of mercury. To fully saturate the stone, it was first placed vertically against the wall of the desiccator, with one edge of the stone partially out of the water, allowing the air to displace as the water rose through the stone. After approximately 4 hr, the stone was knocked over to lie fully submerged in water then occasionally jarred to remove any additional trapped air. The stone was saturated for a minimum of 24 hr prior to testing.

In order to accommodate the height of the loose material in the steel sample ring, a temporary extension was added to prevent material overflow. The temporary extension can be seen in Figure 8b. Figure 8c shows the finished sample prior to saturation. Following sample reconstitution, the height of the specimen was recorded. To become saturated, the specimen, with the top platen, was then placed into a desiccator connected to a pressure panel. De-aired water was added to the desiccator until the water level was just below the top of the specimen. It was critical that the top surface of the specimen be located above the water surface, allowing entrapped air to escape, thereby allowing for full saturation of the specimen. A vacuum pressure of 5.5 in. of mercury was then applied to the desiccator for 12-14 hr.

Figure 8. Fredlund device sample preparation; a) shows sample preparation tools, b) compaction of sample, and c) compacted samples prior to testing.

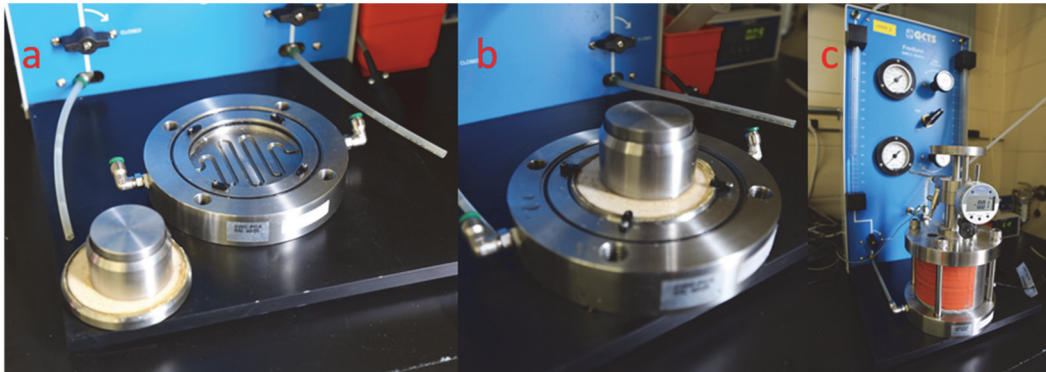


Following the specified saturation time, the sample was removed from the desiccator and the stone was dried to a saturated surface dry state. A saturated mass was recorded, and then the sample was carefully placed into the base of the Fredlund device, as shown in Figures 9a and b. Finally, the steel chamber was fitted and secured to the base (Figure 9c).

The Fredlund device is fitted with a linear variable displacement transducer, which was zeroed following placement of the chamber. Two columns, each attached to a side of the base, were then flushed by forcing air into the top of either the left or the right column until no air bubbles displaced from the base. An initial water level reading was then recorded, followed by another reading after 15-30 min. Typically, by the time the second reading was recorded, the two columns had an equal height of water. Once the two columns were equal, an air pressure increment was applied. Each pressure increment took an average of 8-12 hr to come to equilibrium. Equilibrium in this case is defined as no change in reading for at least 6 hr (GCTS SWC-150 Operating Instructions n.d.). A range of matric suction from 1.5 kPa to 180 kPa was applied by using the Fredlund device. Once the final air pressure attained equilibrium, the device was disassembled, posttest mass and height were recorded, and the water content of the soil was measured.

Twelve sand samples were tested by using the Fredlund device: four samples for each of the reconstituted saturations (18 percent, 24 percent and 30 percent) prepared by using an energy of 200, 300, 600, or 1000 kJ/m<sup>3</sup>. Data reduction was accomplished through a spreadsheet program.

Figure 9. Sample following saturation loaded into Fredlund device.

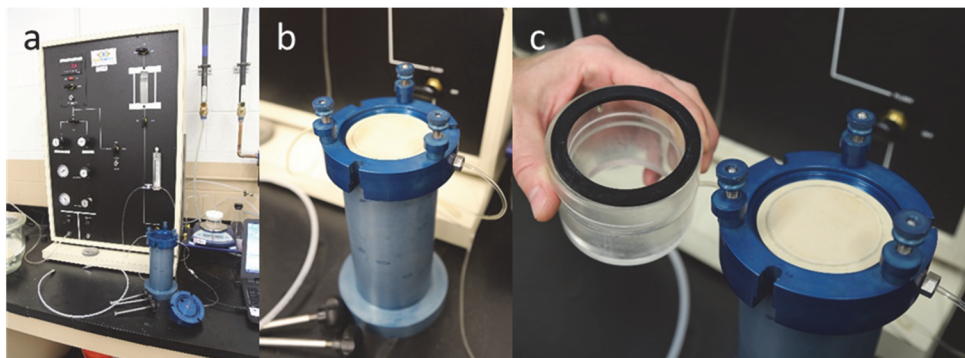


### 2.3 TRIM device

Samples prepared for the TRIM device were constructed inside the TRIM devices acrylic chamber. The chamber has an inside diameter of 6.15 cm and a height of 6.71 cm (with bottom seal). The TRIM device measures the transient outflow response of a sample when two different pressure increments are applied by using axis translation. The outflow data are used as an objective function for a numerical model that solves the Richards equation (Wayllace and Lu 2011).

Prior to sample construction, the bottom stone (a three-bar-high air entry stone) was saturated in the same manner as described for the Fredlund device. The steps for assembling the TRIM chamber are shown in Figure 10. First, the stone was placed into the base of the TRIM chamber (Figure 10b). Next, the seal ring was placed on the bottom of the chamber (Figure 10c) and secured with vacuum grease. The chamber was then fitted down on top of the stone and secured with the three clamps onto the base. Once the chamber was secured, water was flushed through the base to remove air.

Figure 10. TRIM device: (a) disassembled device, (b) stone inserted, and (c) preparing chamber.



The sample was then prepared inside the chamber by adding the loose soil at the prescribed saturation level (Figure 11a), and then compacted by using the prescribed number of blows with the rammer (Figure 11b). Compacted height measurements were recorded for a total of five measurements across the surface of the sample (Figure 11c). Following the height measurements, the top of the chamber was secured in place by three bolts. The TRIM device is fitted with a bubble chamber to allow for the measurement of air that diffuses through the bottom stone. The bubble trap was then filled and an initial height of the water was recorded. The sample was then saturated by applying a vacuum of 10.5 in. of mercury to the top of the specimen, allowing water to flow up from the base and through the specimen. On average, saturation of the sample took 2 hr. Figure 12 shows the assembled chamber as a specimen was being saturated.

**Figure 11. TRIM sample construction: (a) loose soil added to chamber, (b) sample compacted, and (c) height measured.**

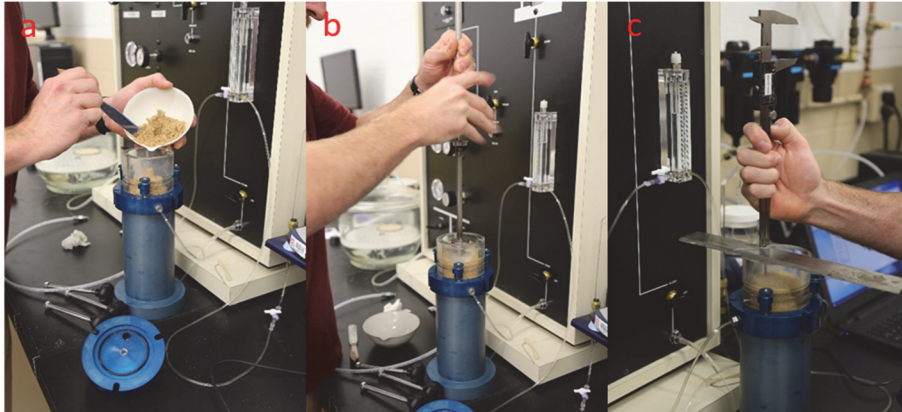
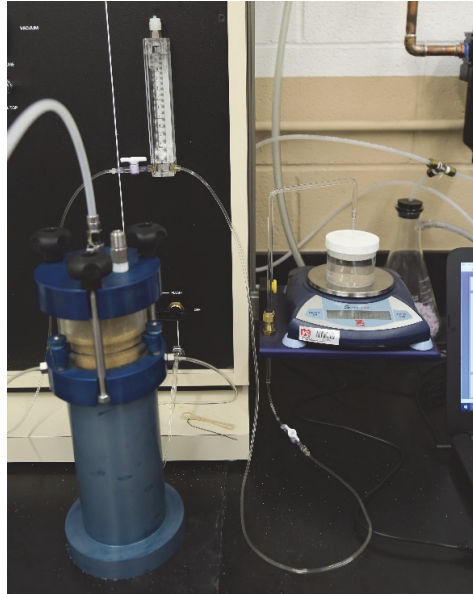


Figure 12. Assembled TRIM chamber and sample saturating.



Following sample saturation, the chamber was then pressurized with a small increment that was just large enough to start water flowing from the chamber to a connected scale. The range of small increments was between 1.5-2.1 kPa. Once equilibrium was reached (i.e., the flow of water from the chamber was near steady state or constant [after a minimum of 24 hr]), a large increment of air pressure was applied to the chamber. The magnitude of the large increment was between 90-100 kPa and reached equilibrium in approximately 48 hr. After 48 hr, the chamber was vented and the base of the chamber was flushed. During flushing, air bubbles evacuated the base and collected in the bubble chamber. Once flushing was complete and no additional air bubbles flowed from the base, the final height of water in the bubble chamber was recorded. The chamber was then disassembled, and the final height of the sample and water content were measured and recorded.

Eighteen samples were tested in the TRIM device. Post processing was accomplished through a proprietary program released through Soil Water LLC. The post processing program fit the measured data by using van Genuchten's model (1980) and also solved for the hydraulic conductivity. All of the samples were tested to attain the drying curve of the SWCC. Samples prepared with 24 percent saturation were tested in duplicate at the same energies as those of the Fredlund device. Because good agreement was found between these duplicates, only one duplicate was performed for the samples prepared at a saturation of 18 percent and 30 percent.

## 2.4 Filter paper test

The filter paper test measured both the matric and total suctions of a sample. The matric suction component was measured by placing a filter paper in contact with the soil sample and letting the water content of the soil sample come to equilibrium with the filter paper. The total suction measurement was achieved through a filter paper placed above the soil sample in a sealed container. The soil water content and the filter paper water content came to equilibrium through vapor flow (Bulut et al. 2001). Testing procedures provided in ASTM D5298 (2010) were followed for measuring soil suction by using Whatman™ number 42 filter papers.

Each filter paper test consisted of a set of eight specimens, all reconstituted at the same energy and saturation. Filter paper tests were completed for each energy (200, 300, 600 and 1000 kJ/m<sup>3</sup>) with a reconstituted saturation of 24 percent. Each specimen was prepared inside polyvinyl chloride (PVC) sample containers with each having both an upper and a lower half. The total height of the PVC sample container (assembled) was 6.52 cm, and the inside diameter was 5.22 cm. The PVC sample containers (Figure 13) were affixed to a porous stone by using epoxy. The filter paper samples were reconstituted in two lifts. After the first lift was constructed, three filter papers were placed on the surface of the first lift (ASTM 2010). The middle filter paper was slightly smaller in diameter than the two outer filter papers. Following construction of the final lift, height measurements were taken. The samples were then placed in a water bath overnight (12-14 hr) to saturate. Following saturation, the samples were removed and placed into an open, well-ventilated room to desaturate. At designated times throughout the desaturation process, a sample was placed in a sealed individual container to attain different water contents in an attempt to define the full SWCC. Desaturation of the final specimen took 3-4 days.

Figure 13. PVC filter paper sample holders.



Before placing each sample into the sealed container, a spacer was placed on top of the specimen. Two filter papers were then placed on top of the spacer to measure the total suction. As each container was sealed with the specimen inside, the containers were placed into a sealed box. Once all eight of the samples had been placed into the sealed box, they were set aside for 14-17 days to reach equilibrium. Once the end of the equilibrium period had been reached, the samples were removed from their respective sealed containers, and the water contents of the soil and filter papers were measured. Poor results were attained by using the PVC sample containers, which possibly did not allow the sample to come to complete equilibrium. A new container was devised by using the same type of porous stone as a base and fixing a #200 mesh screen to the sides. These new sampler containers were 8.29 cm tall and had the same outer diameter as the PVC sample holder's inner diameter. This allowed the new sample containers to use the PVC pipe as a reinforcing member during sample construction. The screen sample containers are shown in Figure 14.

Figure 14. Screen filter paper sample containers.



### 3 Laboratory Testing Results

One of the objectives of this research was to discern how sensitive the fine-grained sand was to variations in soil fabric and density. Taylor et al. (2017) demonstrated that different compactive energies and/or different remolding saturations produce different soil fabrics, resulting in different engineering behavior despite small variations in physical properties. Therefore, the fundamental question of how the SWCC was impacted, if at all, by similar changes was investigated. The variance in soil fabric, and by extension engineering behavior, was represented in terms of the initial remolding saturation (18, 24, and 30 percent) over a wide range of compactive energies (200 to 1,000 kJ/m<sup>3</sup>). The data were fitted with both the van Genuchten and Fredlund and Xing models to determine the shape of the SWCC. The principal difference between the two SWCC models was the post-residual fit behavior, wherein the Fredlund and Xing model has a correction function that forced the SWCC to go through the point 1e6 kPa at zero saturation.

#### 3.1 18 percent saturation

Soils testing on the sand samples prepared at 18 percent saturation consisted of performing nine SWCC tests by using both the TRIM and Fredlund devices. Table 1 shows the pre- and posttest properties of the sample. The initial porosity ( $n_o$ ) and the final porosity ( $n_f$ ) give an idea of the volumetric behavior of the sand during testing. The testing conducted by using the Fredlund device showed that for the samples prepared with 200 and 300 kJ/m<sup>3</sup> there was a contractive behavior, while for the other two samples the behavior was dilative. The samples tested using the TRIM device showed either very little or mostly dilative behavior when pre- and posttest porosities were compared. The initial degree of saturation ( $S_o$ ) shows how close the preparation method was in reaching the target saturation of 18 percent. The minimum saturation at which the samples were prepared was 16.9 percent while the maximum was 18.6 percent, and the mean value was 17.8 percent. All samples fell within 1.1 percent of the target saturation.

Table 1. Soil properties for 18 percent saturation.

Device	prep. energy <sub>3</sub> (kJ/m <sup>3</sup> )	$n_0$	$n_f$	$\gamma_{d,0}$	$\gamma_{d,f}$	$S_0$	$S_f$	$k_{sat}$ (cm/s)
Fredlund	200	0.385	0.359	103.67	108.04	17.78%	3.78%	NA
	300	0.380	0.372	104.48	105.81	17.79%	4.40%	
	600	0.369	0.371	110.51	106.90	18.55%	4.23%	
	1000	0.380	0.484	104.49	86.88	16.90%	2.32%	
TRIM	200	0.387	0.387	103.25	103.22	17.64%	8.87%	0.28
	200	0.395	0.415	101.96	98.50	17.27%	3.48%	0.25
	300	0.383	0.426	103.95	96.65	17.81%	5.86%	0.20
	600	0.378	-	104.73	-	17.63%	-	0.33
	1000	0.373	0.405	105.62	100.31	18.44%	8.47%	0.27

The results of the SWCC testing are shown in Figures 15 and 16 with the data fitted using the van Genuchten and Fredlund and Xing models, respectively. The legends are labeled according to the material (i.e., SP) followed by the saturation level (18), the preparation energy, and either an “F” (Fredlund) or a “T” (TRIM). The results of the Fredlund data are translated approximately 2 kPa higher than the TRIM device data irrespective of model fit. In general, there is good agreement between the two data sets. The Fredlund and Xing model matches the data near the residual point better than the van Genuchten model but has nearly the same results prior to the residual point.

Figure 15. Sand samples prepared at 18 percent saturation fitted with the van Genuchten model.

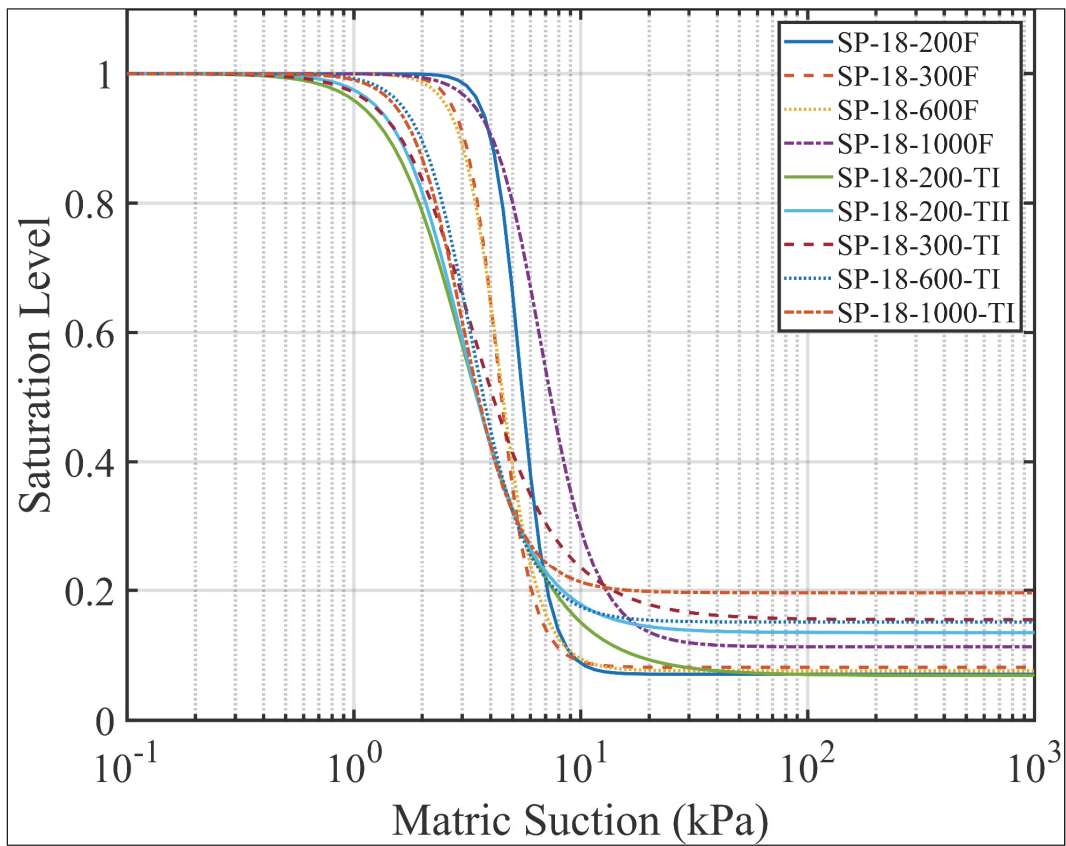


Figure 16. Sand samples prepared at 18 percent saturation fitted with the Fredlund and Xing model.

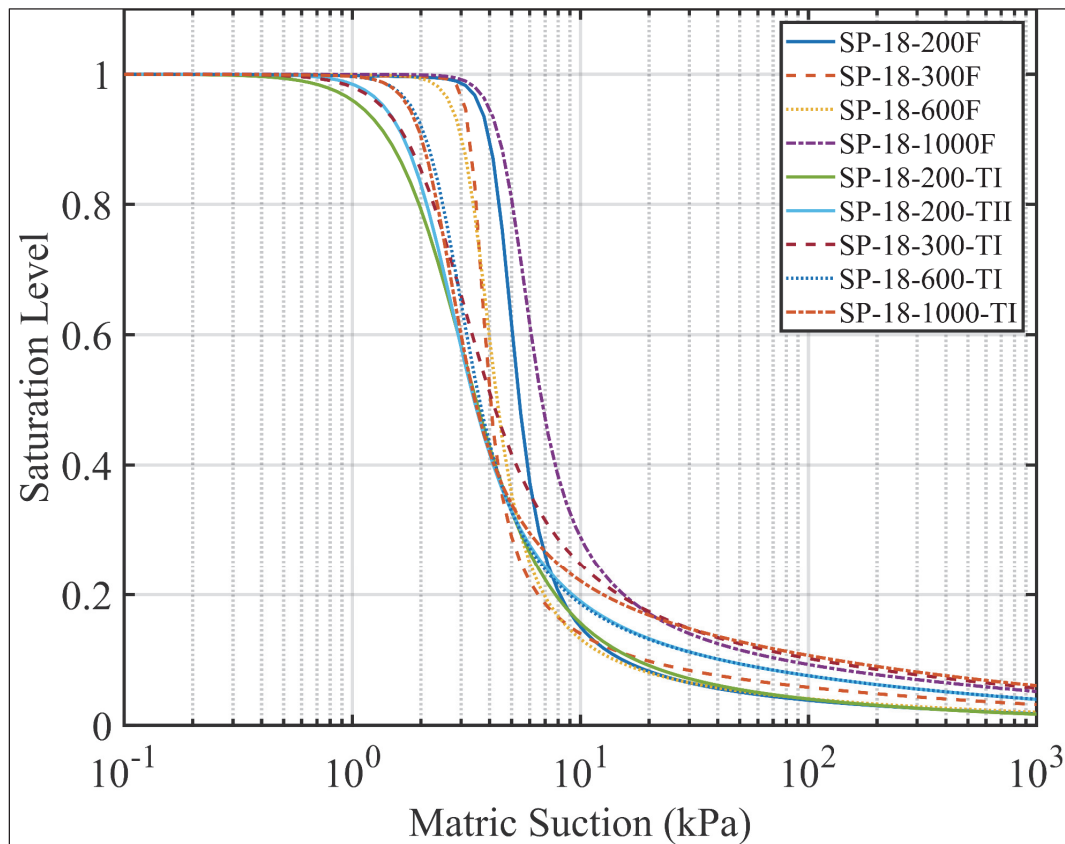


Table 2 shows the model parameters for both the van Genuchten and the Fredlund and Xing models. The van Genuchten model parameter residual saturation shows a slight increase with increasing preparation energy, while most of the other parameters show very little sensitivity to preparation energy. The slope of the post-AEV SWCC is greater for the Fredlund device than for the TRIM device, and the  $n$  parameter for the van Genuchten model decreases with increasing preparation energy. The parameter  $m$  for the van Genuchten model is not presented because the relationship  $m=1-1/n$  was assumed. The residual matric suction value for the Fredlund and Xing model was based on the residual water content value and corresponding suction from the van Genuchten model.

Table 2. SWCC model data for sand samples prepared at 18 percent saturation.

Device	prep. energy <sup>3</sup> (kJ/m <sup>3</sup> )	van Genuchten model				Fredlund and Xing model				
		$\theta_r$	$\theta_s$	$\alpha$ (1/kPa)	$n$	$\theta_s$	$a$ (kPa)	$n$	$m$	$\psi_r$
Fredlund	200	0.03	0.38	0.19	7.24	0.38	4.52	9.44	0.93	45.00
	300	0.03	0.38	0.24	6.27	0.38	3.45	16.48	0.68	52.00
	600	0.03	0.38	0.24	5.47	0.38	3.50	7.78	0.96	114.00
	1000	0.04	0.38	0.16	4.15	0.37	4.98	7.28	0.76	348.00
TRIM	200	0.03	0.39	0.39	2.78	0.39	2.48	2.75	1.36	147.00
	200	0.05	0.39	0.38	3.24	0.39	2.22	3.93	0.93	135.00
	300	0.06	0.38	0.36	2.82	0.38	2.37	3.25	0.90	349.00
	600	0.06	0.38	0.33	4.00	0.38	2.51	5.51	0.82	57.00
	1000	0.07	0.37	0.36	4.03	0.37	2.27	6.24	0.67	50.00

Due to the data variability's being primarily attributed to the testing method (i.e., TRIM or Fredlund) and not a function of compactive effort, maximum and minimum boundaries were determined to encapsulate all the data. Figures 17 and 18 show the resulting mean and median values of the SWCC, irrespective of test apparatus or compactive energy, depending on the model fit (i.e, the van Genuchten or the Fredlund and Xing model). The resulting mean SWCC is then considered the "true" or realistic SWCC for this material at the given remolding saturation of 18 percent depending on model fit used.

Figure 17. Maximum, minimum, mean, and median SWCC data for samples prepared at a saturation of 18 percent, van Genuchten model.

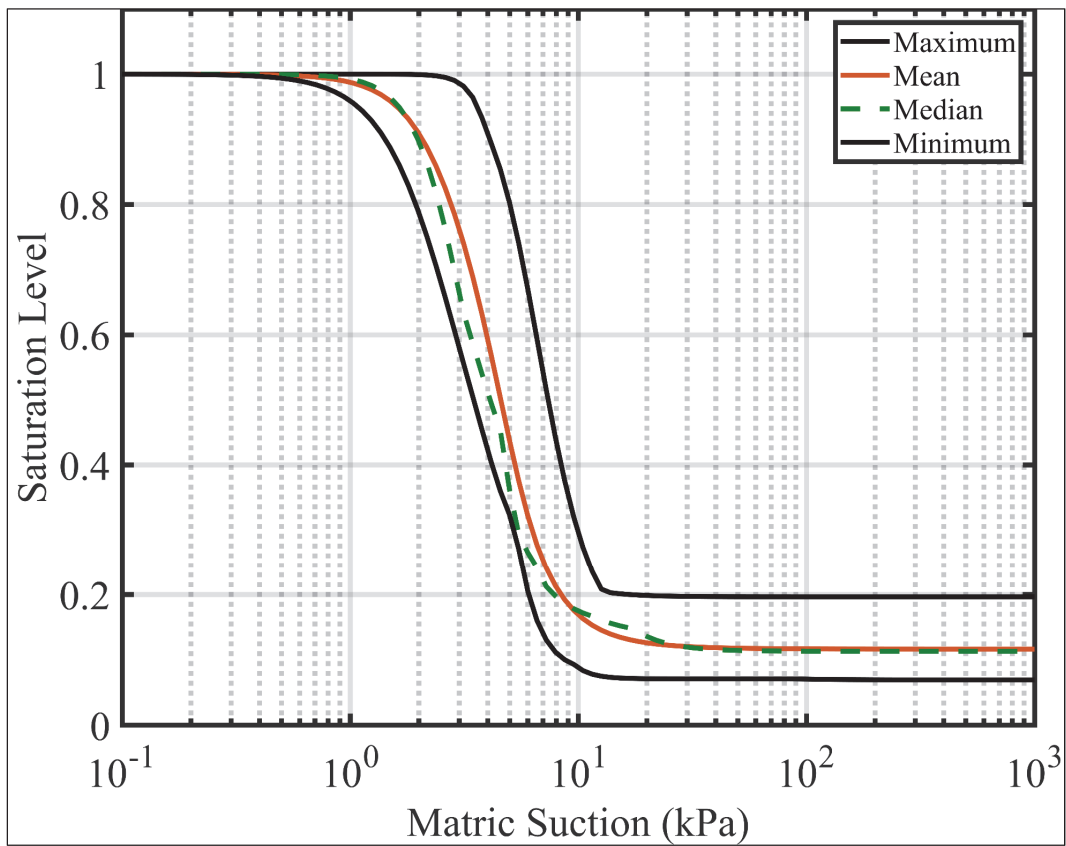
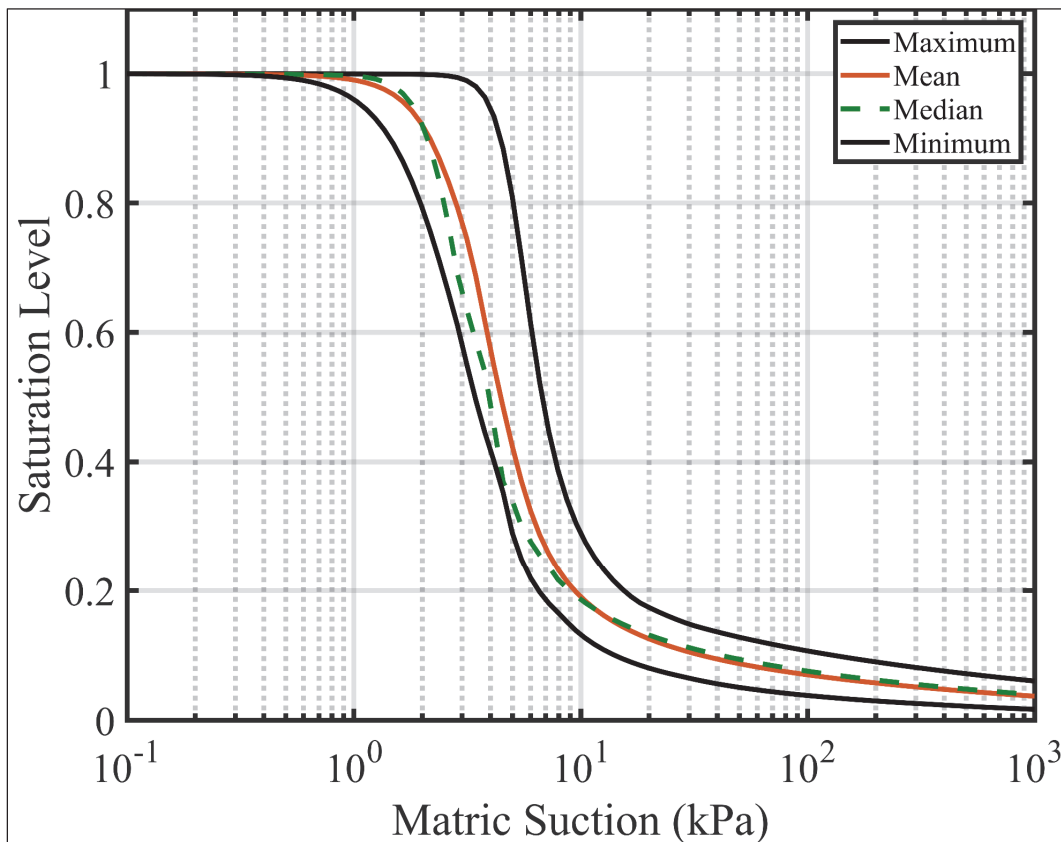


Figure 18. Maximum, minimum, mean, and median SWCC data for samples prepared at a saturation of 18 percent, Fredlund and Xing model.



### 3.2 24 percent saturation

Samples prepared with a degree of saturation of 24 percent were tested using the Fredlund device, TRIM, and FPM. The target saturation of these samples was 24 percent. The maximum degree of saturation for a prepared sample was 24.95 percent, the minimum was 22.01 percent, and the mean was 23.43 percent (Table 3). These were all acceptable in accordance with required tolerances outlined by Taylor et al. (2017). Unlike the 18 percent saturation specimens, the pre- and post-test porosities all exhibited dilatancy during SWCC testing. The saturated hydraulic conductivity shown in the  $k_{sat}$  column ranged from 0.18 to 0.31 cm/s, and the mean value was 0.27 cm/s. The hydraulic conductivity values were acquired through the postprocessing of the TRIM device data.

Table 3. Soil properties for 24 percent saturation.

Device	prep. energy (kJ/m <sup>3</sup> )	$n_o$	$n_f$	$\gamma_{d,o}$	$\gamma_{d,f}$	$S_o$	$S_f$	$k_{sat}$ (cm/s)
Fredlund	200	0.378	0.378	104.73	104.75	24.08%	4.24%	NA
	300	0.379	0.435	104.62	95.15	23.94%	2.27%	
	600	0.380	0.434	104.44	95.43	23.11%	2.67%	
	1000	0.359	0.360	108.07	107.77	24.71%	4.50%	
TRIM	200	0.395	0.417	101.91	98.27	23.02%	5.24%	0.31
	200	0.375	0.409	105.26	99.54	24.95%	5.48%	0.30
	300	0.395	0.413	101.96	104.22	22.53%	4.49%	0.18
	300	0.394	0.431	102.08	95.92	22.45%	2.41%	0.27
	600	0.381	0.381	104.33	104.33	23.34%	5.68%	0.30
	600	0.390	0.406	102.78	100.01	22.01%	4.94%	0.30
	1000	0.375	0.403	105.37	100.59	23.05%	7.32%	0.25
	1000	0.369	0.397	106.3	101.63	23.96%	7.25%	0.25

Figure 19 shows the results of the SWCC testing for both the TRIM and the Fredlund devices fitted with the van Genuchten model. The legend in Figure 19 has the same configuration as that described for the samples prepared at 18 percent saturation. There is less of a pronounced difference between the TRIM and the Fredlund device results, although a difference is still present with the Fredlund device results plotting slightly to the right (higher matric suction values) of the TRIM device results. The slope of the Fredlund device data is also steeper than that of the TRIM results. This indicates that the samples tested with the Fredlund device desaturate at a smaller range of matric suctions. Figure 20 shows the results of the SWCC testing using both the TRIM and the Fredlund devices for samples prepared using 24 percent saturation. There is relatively good agreement between the Fredlund and TRIM devices with little more than a 2 kPa difference between the maximum and minimum measured SWCC. As with the 18 percent saturation specimens, the data variance is predominately influenced by the testing method and not by the compactive energy (i.e., density state).

Figure 19. Sand samples prepared at 24 percent saturation fitted with the van Genuchten model.

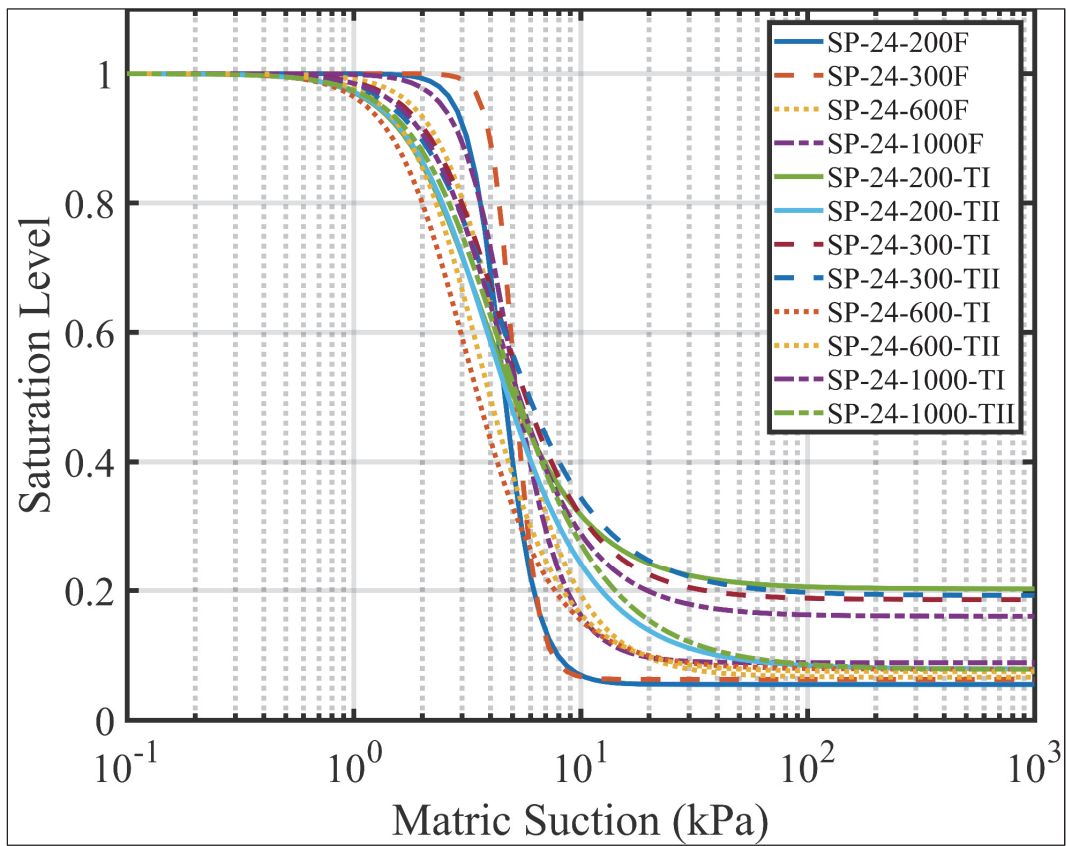


Figure 20. Sand samples prepared at 24 percent saturation fitted with the Fredlund and Xing model.

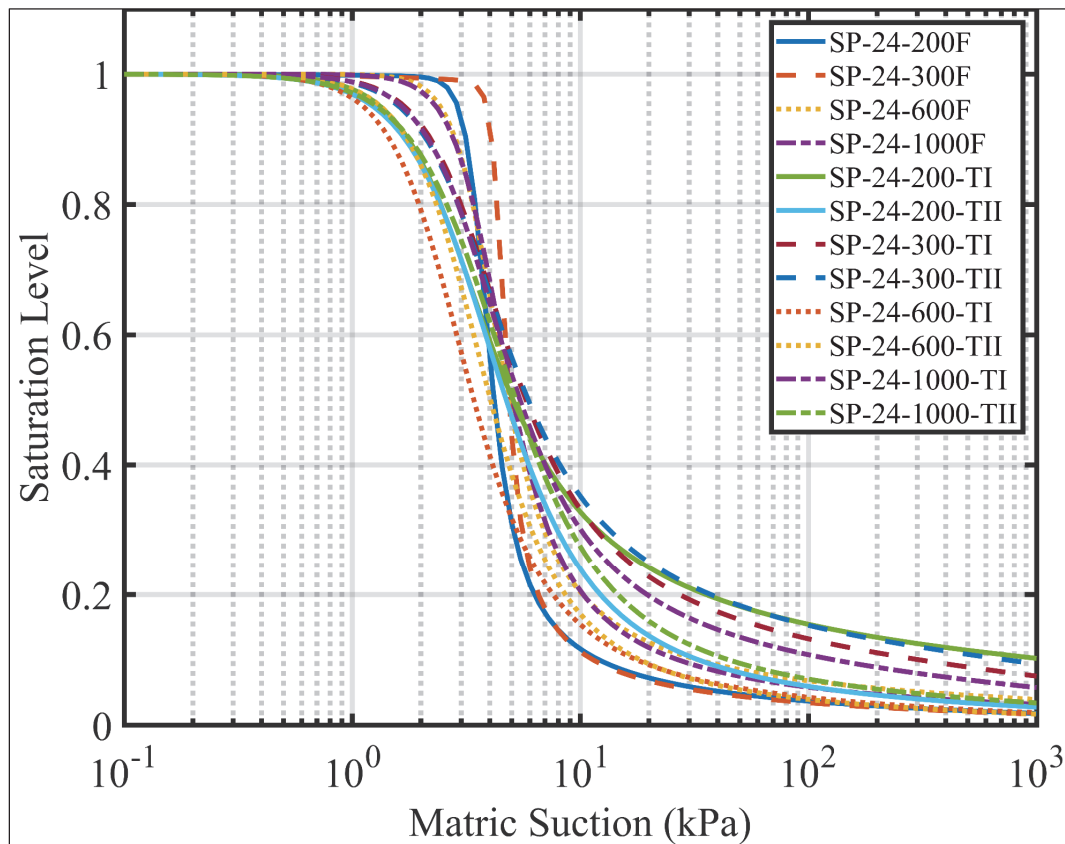


Table 4 shows the results of the SWCC testing on the samples prepared at a 24 percent saturation level. Both the van Genuchten and the Fredlund and Xing model parameters are shown. The  $n$  parameter for both models is larger for the Fredlund device results than for the TRIM results; this agrees with the observation that the SWCC curves are slightly steeper for the Fredlund device curves. The  $\alpha$  parameters for the Fredlund device range between 0.2 and 0.31 1/kPa with no apparent relationship to preparation energy. The same is true for the Fredlund and Xing  $\alpha$  parameter.

Table 4. SWCC model data for sand samples prepared at 24 percent saturation.

Device	prep. energy (kJ/m <sup>3</sup> )	van Genuchten				Fredlund and Xing				
		$\vartheta_r$	$\vartheta_s$	$\alpha$ (1/kPa)	$n$	$\vartheta_s$	$a$ (kPa)	$n$	$m$	$\psi_r$
Fredlund	200	0.02	0.38	0.23	6.05	0.38	3.52	9.98	0.91	63.00
	300	0.02	0.38	0.20	8.89	0.38	4.34	17.74	0.80	30.00
	600	0.03	0.39	0.25	3.14	0.39	3.50	5.16	0.94	2275.00
	1000	0.03	0.35	0.22	4.17	0.36	3.67	4.40	1.06	3000.00
TRIM	200	0.08	0.40	0.34	2.56	0.40	2.40	2.84	0.79	5000.00
	200	0.03	0.38	0.31	2.50	0.38	3.14	2.39	1.33	1180.00
	300	0.07	0.39	0.27	2.80	0.39	3.05	3.01	0.85	490.00
	300	0.08	0.39	0.29	2.53	0.39	2.88	2.90	0.80	1069.00
	600	0.03	0.38	0.38	2.87	0.38	2.41	2.89	1.31	266.00
	600	0.03	0.39	0.33	2.95	0.39	2.94	2.88	1.38	379.00
	1000	0.06	0.37	0.28	2.79	0.37	3.10	2.98	0.94	386.00
	1000	0.03	0.37	0.29	2.42	0.37	3.31	2.31	1.28	1712.00

In the same manner as the 18 percent saturation samples, the 24 percent remolding saturation specimen data were bound (Figures 21 and 22) and the mean and median SWCC results calculated for the van Genuchten and Fredlund and Xing models.

Figure 21. Maximum, minimum, mean, and median SWCC data for samples prepared at a saturation of 24 percent, van Genuchten model.

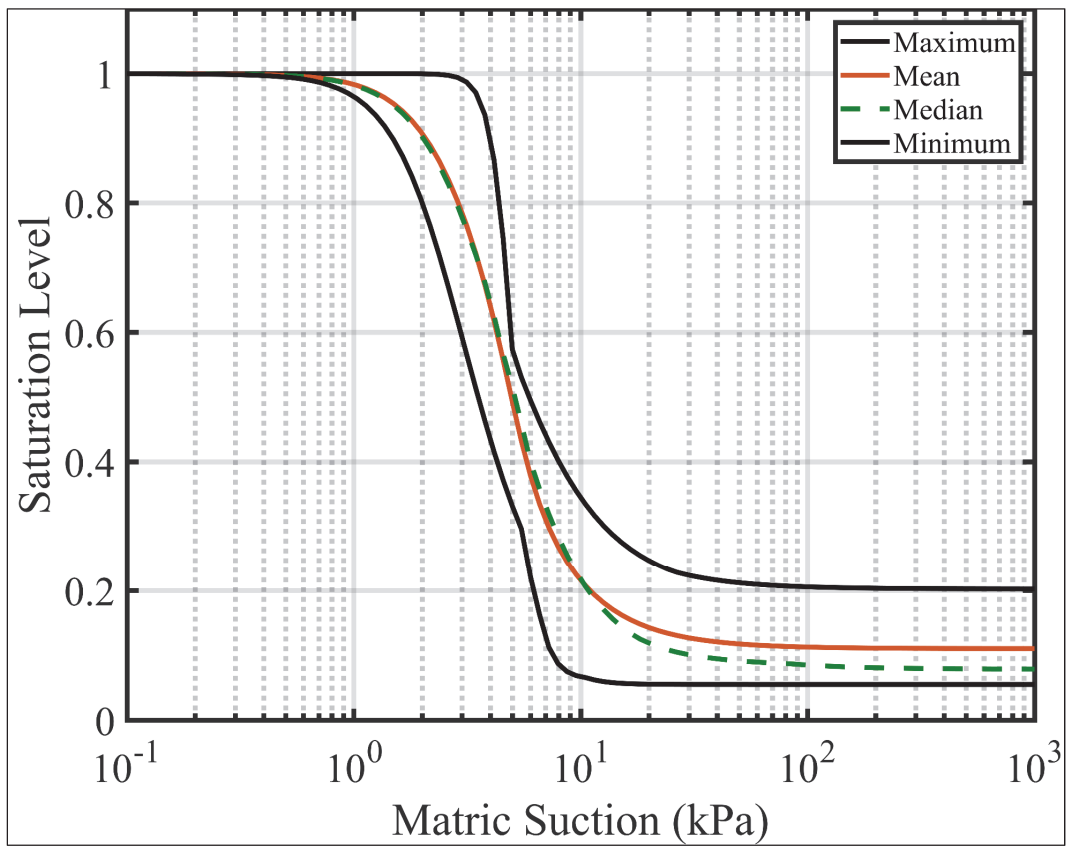
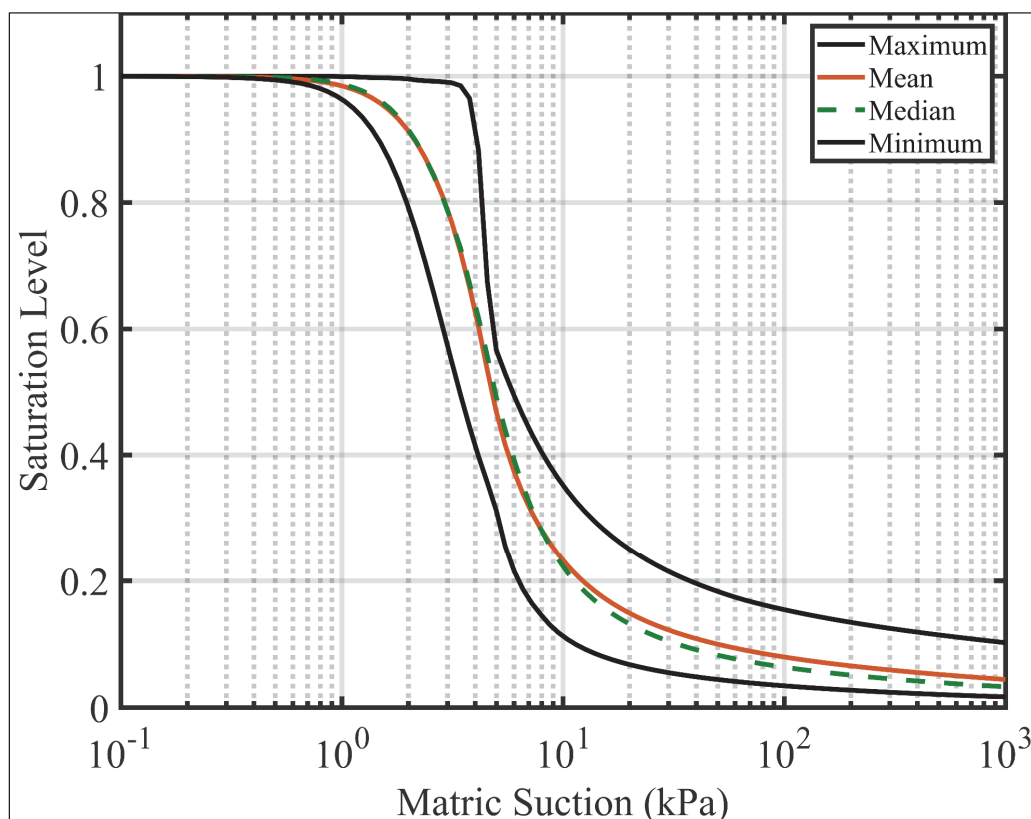


Figure 22. Maximum, minimum, mean, and median SWCC data for samples prepared at a saturation of 24 percent, Fredlund and Xing model.



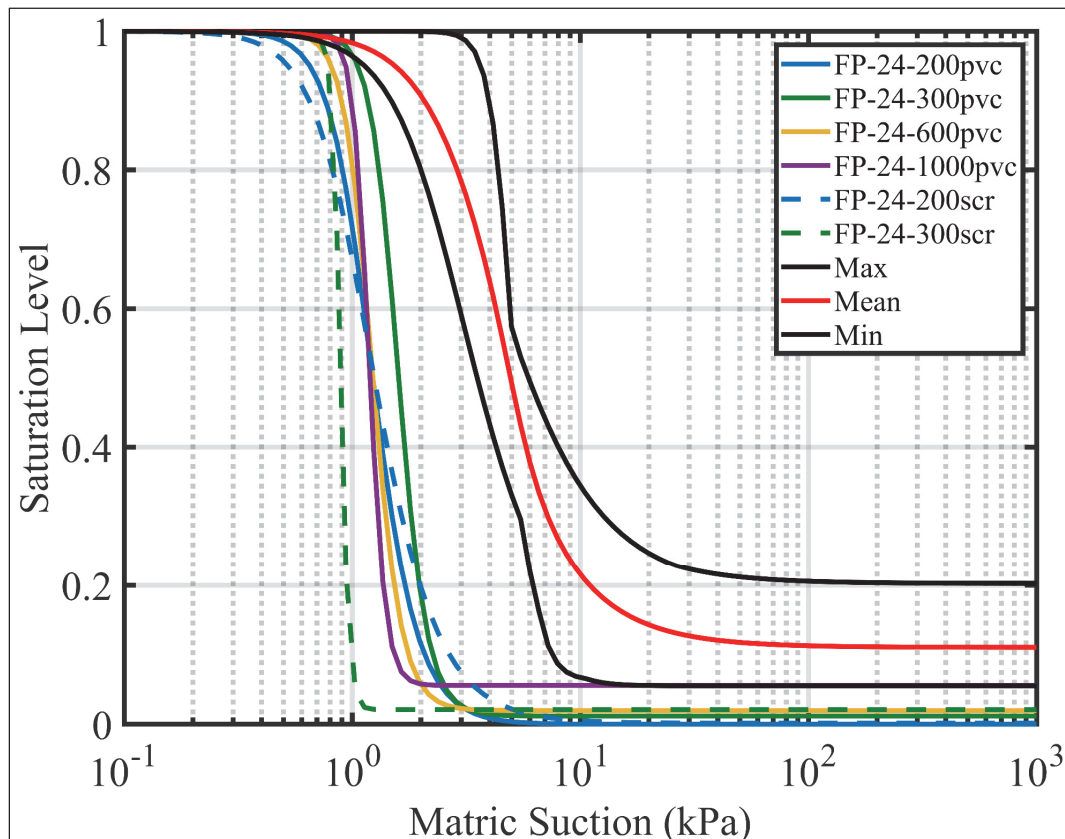
Filter paper specimens were prepared at the 24 percent saturation level. Six tests were performed in total at 200, 300, 600, and 1000 kJ/m<sup>3</sup> by using the PVC sample holders. Two additional tests were performed by using the #200 screen sample holders. Each sample was prepared for eight specimens at different energy levels to acquire a representative SWCC; each specimen was dried at a different time period. Table 5 shows the van Genuchten and Fredlund and Xing model parameters, which were fitted to the testing data.

Table 5. Model parameters for the FPM results.

prep. energy (kJ/m <sup>3</sup> )	van Genuchten				Fredlund and Xing				
	$\vartheta_r$	$\vartheta_s$	$\alpha$ (1/kPa)	$n$	$\vartheta_s$	$\alpha$ (kPa)	$n$	$m$	$\psi_r$
200PVC	0.00	0.38	0.87	4.80	0.39	14.16	2.86	2005.21	1500.00
300PVC	0.005	0.39	0.65	7.33	0.39	1.60	6.56	2.54	1500.00
600PVC	0.008	0.38	0.84	7.24	0.38	1.09	62.82	0.80	1500.00
1000PVC	0.021	0.38	0.85	12.49	0.38	1.11	20.83	1.03	1500.00
200scr	0.001	0.40	0.92	3.56	0.40	32.10	2.22	2415.33	1500.00
300scr	0.009	0.41	1.13	24.60	0.41	0.85	52.03	0.80	1500.00

The results of the FPM did not correspond well to the results of Fredlund or TRIM. The FPM results (Figure 23) showed some variation from test to test but overall did not seem to correspond well to the rest of the data set from the van Genuchten model fit shown in Figure 23. The FPM results plot approximately one order of magnitude smaller than the other device results and were deemed to be inaccurate over the range of matric suctions for this material. Considering the calibration curve presented in ASTM 5298 (2010), small changes in water content for filter paper water contents greater than 45 percent yielded small changes in matric suction due to a change in slope of the calibration curve. The SWCC for a sandy material is expected to result in large changes in water content over small changes in matric suction. The calibration curve presented in ASTM 5298 (2010) does not exceed a filter paper water content of 90 percent and a majority of the results of the filter paper testing exceeded 90 percent, indicating that the prescribed calibration curve would not be acceptable. A majority of the filter paper water content values for the fine sand tests exceeded 90 percent. Therefore, no further testing using the FPM was performed on this material.

Figure 23. Results of FPM compared to Fredlund and TRIM device mean, maximum, and minimum data.



### 3.3 30 percent saturation

Table 6 shows the soil properties for samples prepared at 30 percent saturation. All of the soils exhibit dilative behavior when the pre- and posttest porosity values are compared. The maximum saturation of the prepared samples was 31.5 percent, and the minimum saturation level was 28.93 percent with the mean value of 29.69 percent. The mean saturated hydraulic conductivity was 0.3 cm/s with maximum and minimum values of 0.36 and 0.25 cm/s, respectively, as computed from the TRIM device data reduction.

Table 6. 30 percent saturation soil properties.

Device	Prep. energy (kJ/m <sup>3</sup> )	$n_o$	$n_f$	$V_{d,o}$	$V_{d,f}$	$S_o$	$S_f$	$k_{sat}$ (cm/s)
Fredlund	200	0.390	0.390	102.73	102.86	29.10%	2.02%	NA
	300	0.383	0.384	103.93	103.7	29.82%	3.31%	
	600	0.376	0.391	105.12	102.67	29.32%	4.31%	
	1000	0.360	0.378	103.38	104.8	31.50%	64.35%	
TRIM	200	0.390	0.414	102.84	98.66	29.91%	4.19%	0.26
	300	0.388	0.426	103.06	96.66	29.20%	5.72%	0.36
	600	0.383	0.410	103.95	99.38	28.93%	6.63%	0.25
	1000	0.373	0.398	105.71	101.51	29.71%	7.41%	0.33

The results of the Fredlund and TRIM tests fit for both the van Genuchten and Fredlund and Xing models using the fit parameters in Table 7 and illustrated in Figures 24 and 25, respectively. As observed with other remolding saturations, the TRIM device SWCC falls to the left of the Fredlund device data. This is more than likely due to the way in which the TRIM device indirectly measures the SWCC through inverse modeling of two pressures while the Fredlund device directly measures each point, and a model is fit to the data following testing.

Figure 24. Sand samples prepared at 30 percent saturation fitted with the van Genuchten model.

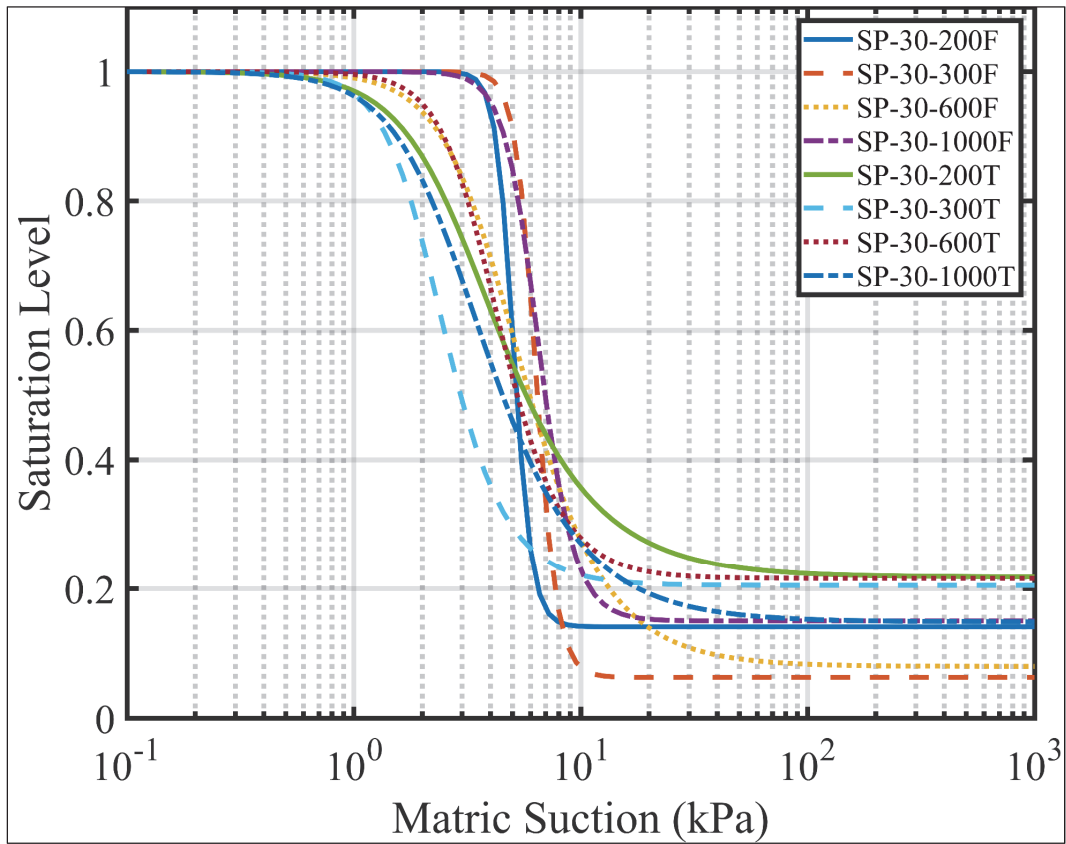
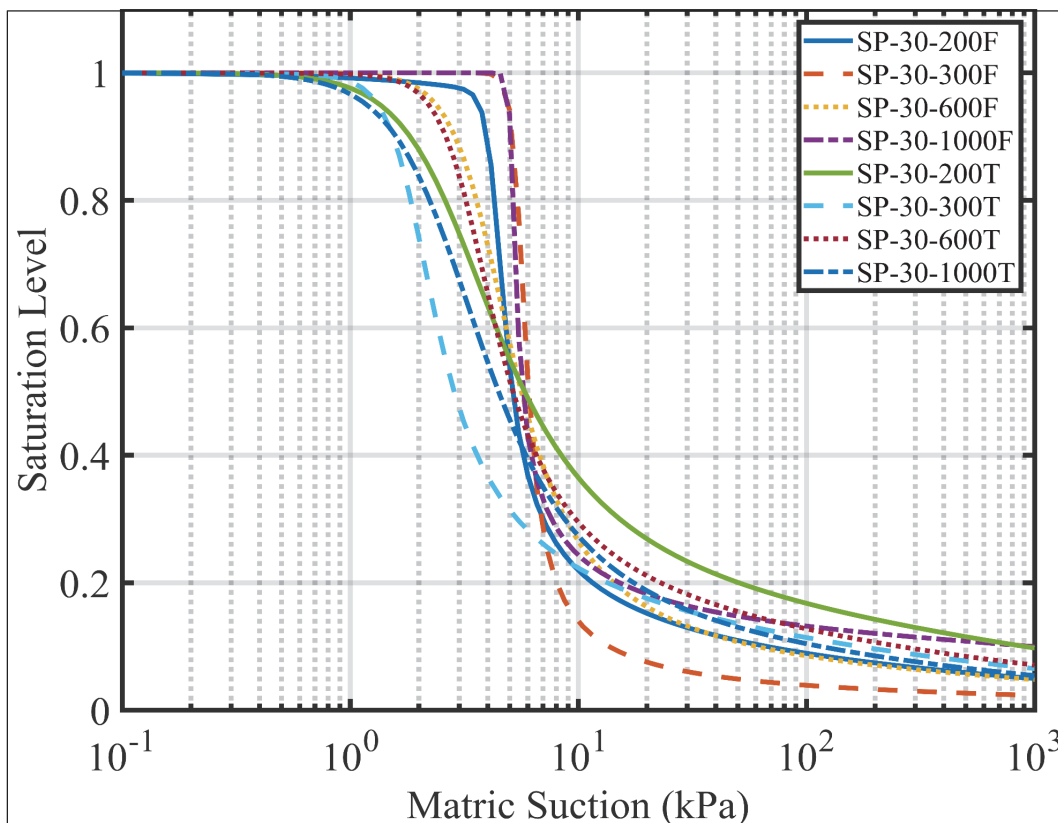


Figure 25. Sand samples prepared at 24 percent saturation fitted with the Fredlund and Xing model.



The Fredlund device sample testing at an energy level of 1000 kJ/m<sup>3</sup> has a d (drying) and w (wetting) following the energy level in Table 7. This test was run through the drying pressures, and then the air pressure was reduced in increments to test for the wetting SWCC.

Table 7. SWCC model data for sand samples prepared at 30 percent saturation.

Device	prep. energy (kJ/m <sup>3</sup> )	van Genuchten				Fredlund and Xing				
		$\theta_r$	$\theta_s$	$\alpha$ (1/kPa)	$n$	$\theta_s$	$a$ (kPa)	$n$	$m$	$\psi_r$
Fredlund	200	0.05	0.39	0.20	11.16	0.39	4.21	15.51	0.56	10.00
	300	0.02	0.38	0.16	9.74	0.38	5.42	18.55	0.81	3000.00
	600	0.03	0.40	0.23	2.79	0.39	3.74	4.12	0.94	1500.00
	1000d	0.06	0.40	0.16	5.95	0.39	5.06	46.06	0.41	3000.00
	1000w	0.06	0.38	0.22	4.90	0.38	4.07	47.84	0.41	3000.00
TRIM	200	0.09	0.39	0.33	2.42	0.39	2.53	2.63	0.77	285.00
	300	0.08	0.39	0.46	3.56	0.39	1.75	5.52	0.65	30.00
	600	0.08	0.38	0.26	3.62	0.38	3.09	4.78	0.70	80.00
	1000	0.06	0.37	0.36	2.50	0.37	2.43	2.63	0.97	210.00

In the same manner as the 18 percent and 24 percent remolding saturation samples, the 30 percent specimen data were bound (Figures 26 and 27), and the mean and median SWCC results were calculated for the van Genuchten and Fredlund and Xing models.

Figure 26. Maximum, minimum, mean, and median SWCC data for samples prepared at a saturation of 30 percent, van Genuchten model.

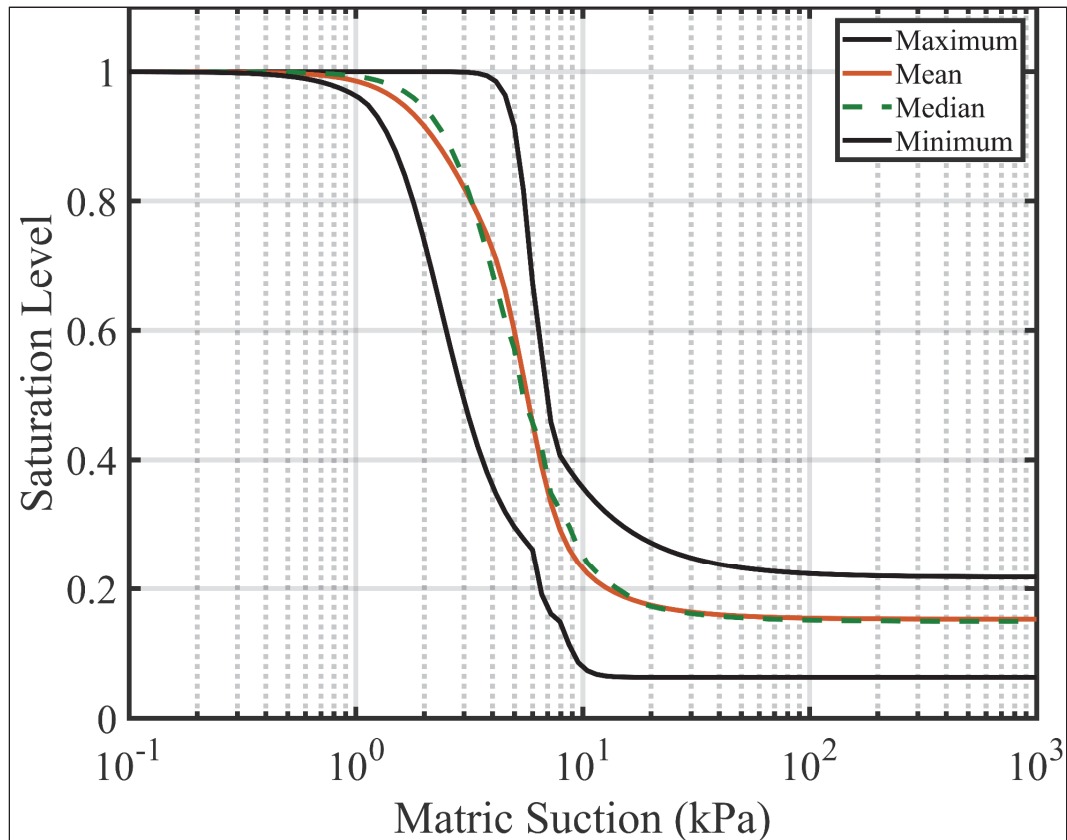
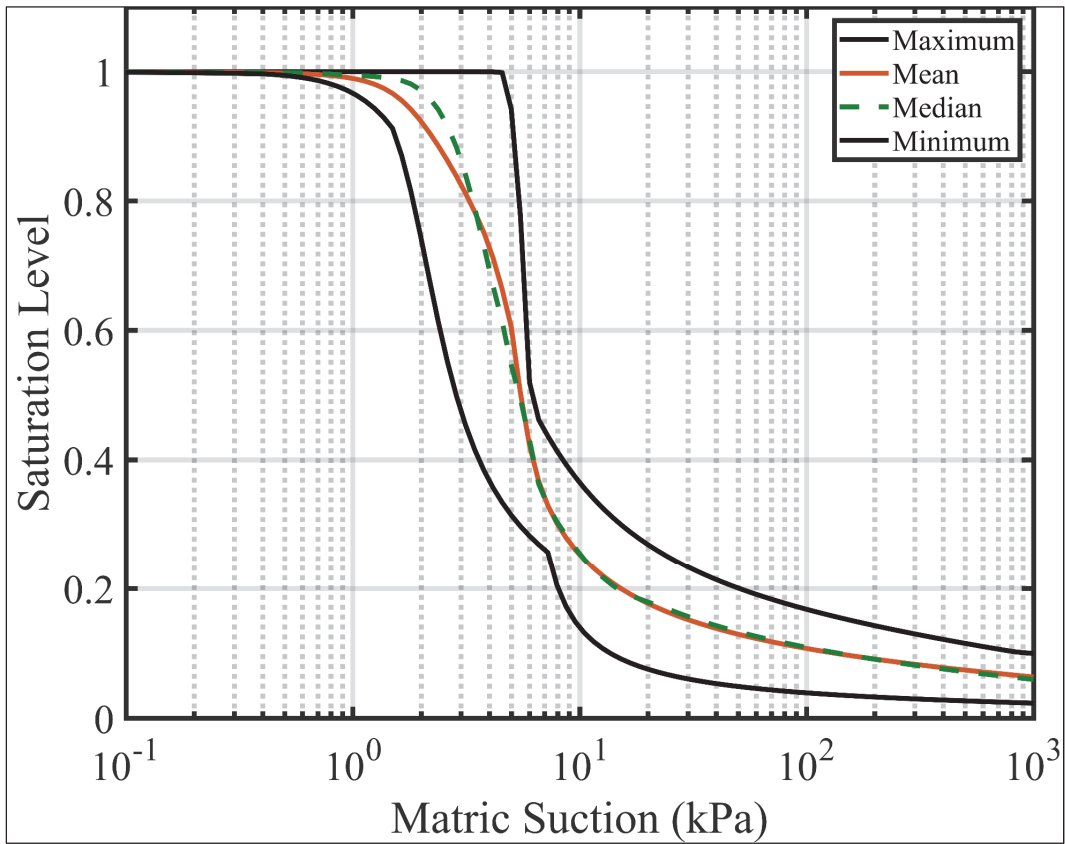


Figure 27. Maximum, minimum, mean, and median SWCC data for samples prepared at a saturation of 30 percent, Fredlund and Xing model.



## 4 Discussion

To predict or model the behavior of unsaturated soils, one of the primary constitutive components required is the SWCC. However, the true sensitivity of the SWCC, for predictive purposes, is not well-understood. This is especially true for cohesionless soils. Thus, a goal of this investigation was to investigate the effects of testing procedures, model fits, and soil fabric variability on the construction of an SWCC for a poorly graded fine sand that is representative of an SP material. Preparation of samples was performed by using the technique outlined by Taylor et al. (2017), which controls soil mass, compactive energy, and reconstitution saturation to provide tight controls that resulted in samples being within 2 percent of tolerances. This preparation and sample repeatability was crucial to reducing (or statistically eliminating) testing uncertainty unrelated to the aforementioned independent variables (e.g., testing procedures, model fits, and soil fabric variability). Samples were prepared at three different saturation levels (18, 24, and 30 percent) that were all dry of optimum, over a range of compactive energies (Table 8). Each compactive energy yielded a different soil fabric, as indicated through the void ratio,  $e$ , in Table 8. However, it is observed that the void ratio is consistent with variable saturation for a fixed-compactive energy. Taylor et al. (2017) showed that despite a consistent void ratio and fixed-compactive energy, variation engineering behavior, both volumetric and strength behavior, occurs at different degrees of remolding saturation, as the soil fabric is not equivalent.

Table 8. Variation in soil density state for the reconstituted specimens.

Compactive Effort (kJ/m <sup>3</sup> )	SAT 18%		SAT 24%		SAT 30%	
	Gravimetric Water Content	$e$	Gravimetric Water Content	$e$	Gravimetric Water Content	$e$
200	4.19%	0.629	5.59%	0.629	6.98%	0.628
400	4.06%	0.609	5.42%	0.610	6.77%	0.609
600	3.99%	0.599	5.32%	0.599	6.65%	0.599
800	3.94%	0.591	5.25%	0.591	6.56%	0.590
1000	3.90%	0.585	5.20%	0.585	6.50%	0.585

From the SWCC results (see Section *Laboratory Testing Results* Figures 15, 16, 19, 20, 24, and 25) for each remolding saturation, changes in void ratio have a minimal impact on the SWCC model fit and laboratory

data scatter compared with the testing procedure (e.g., Fredlund, TRIM, or filter paper).

The mean curves, shown in Figure 28, were calculated from saturation levels ranging from saturated to dry (post residual) and fit using the van Genuchten model (see Section *Laboratory Testing Results*, Figures 17, 21, and 26).

Figure 28. Mean SWCC's for 18, 24 and 30 percent saturation levels.

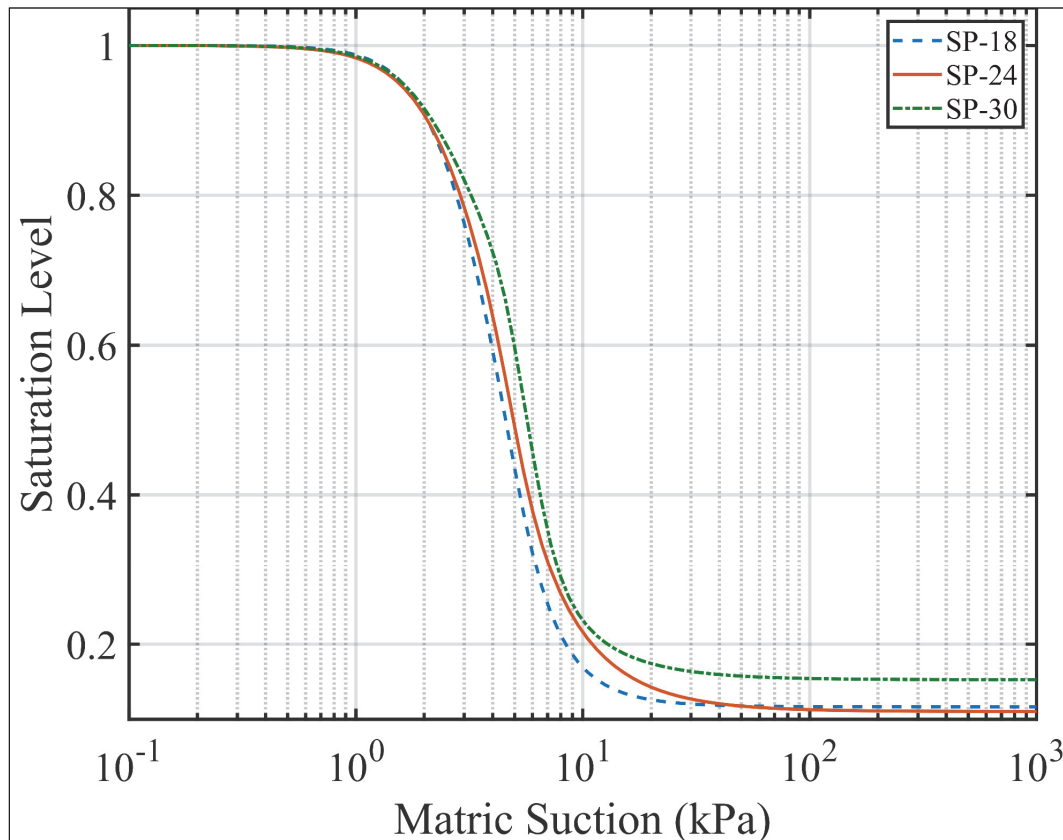


Figure 28 illustrates very little difference between the mean curves, although a slight increase in saturation level occurring post-AEV can be seen as the reconstituted saturation increases. Unlike the engineering behavior variance observed by Taylor et al. (2017) for different remolding saturations, the SWCC for this material is statistically unaffected by changes to the void ratio, remolding saturation, and compactive energy. Figures 29, 30, and 31 show the variance associated with the SWCC testing at each reconstituted saturation level across the four compactive energy levels (200, 300, 600, and 1000 kJ/m<sup>3</sup>).

Figure 29. Variance across preparation energies for samples prepared at 18 percent saturation level.

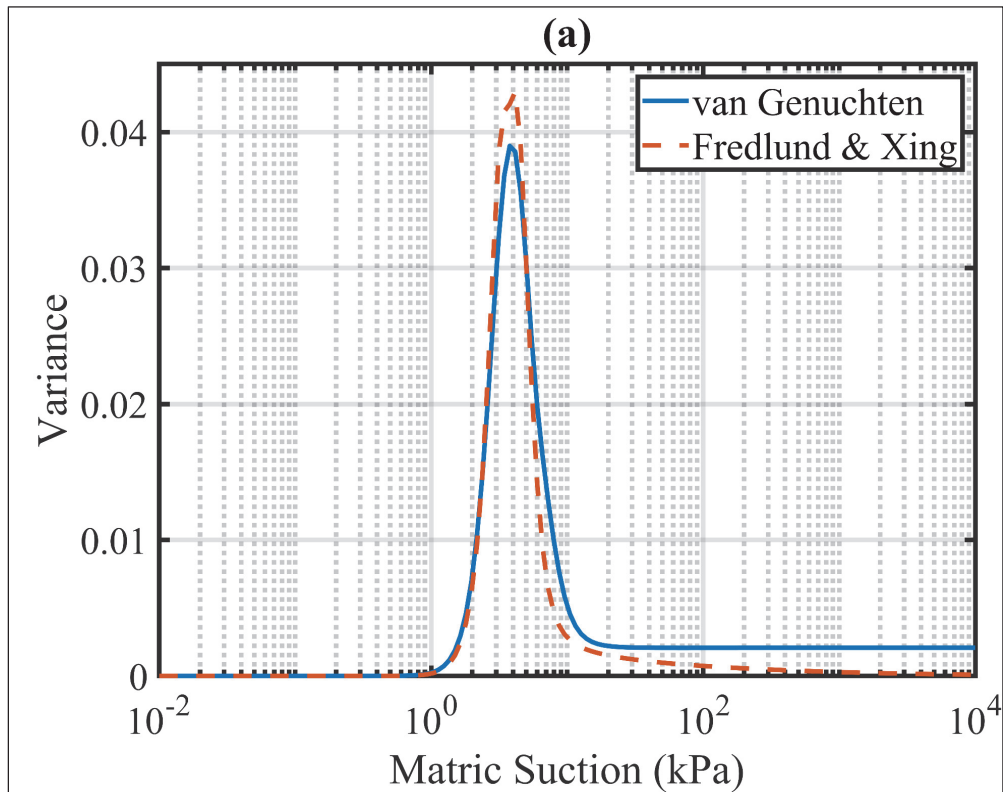


Figure 30. Variance across preparation energies for samples prepared at 24 percent saturation level.

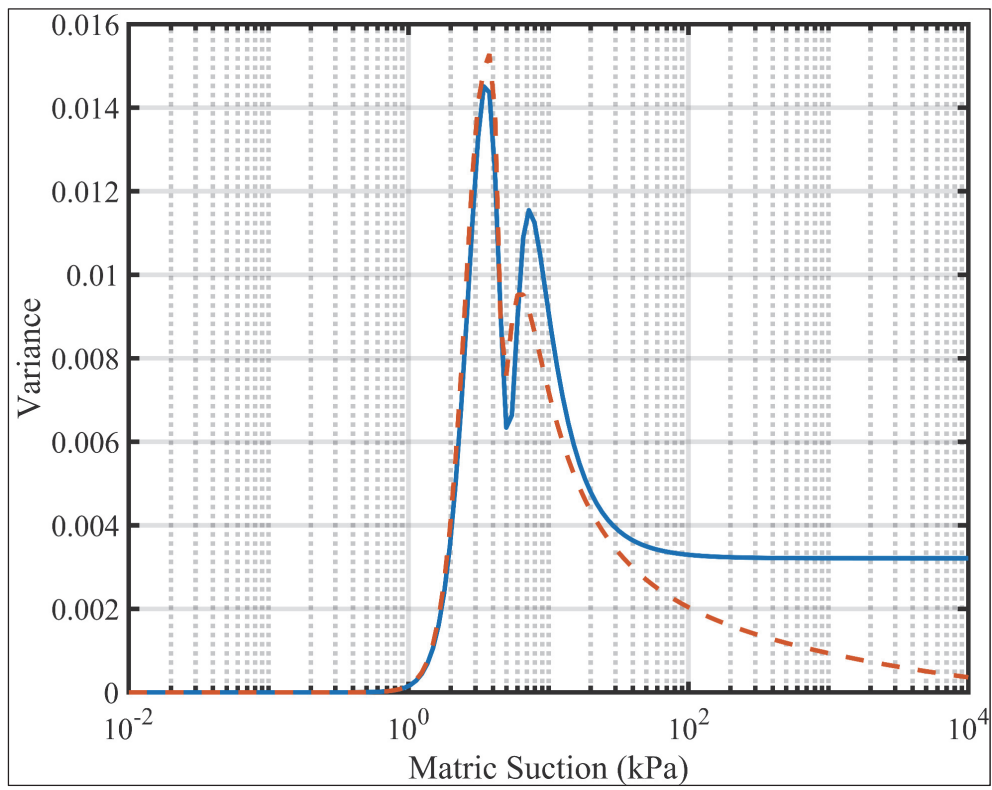
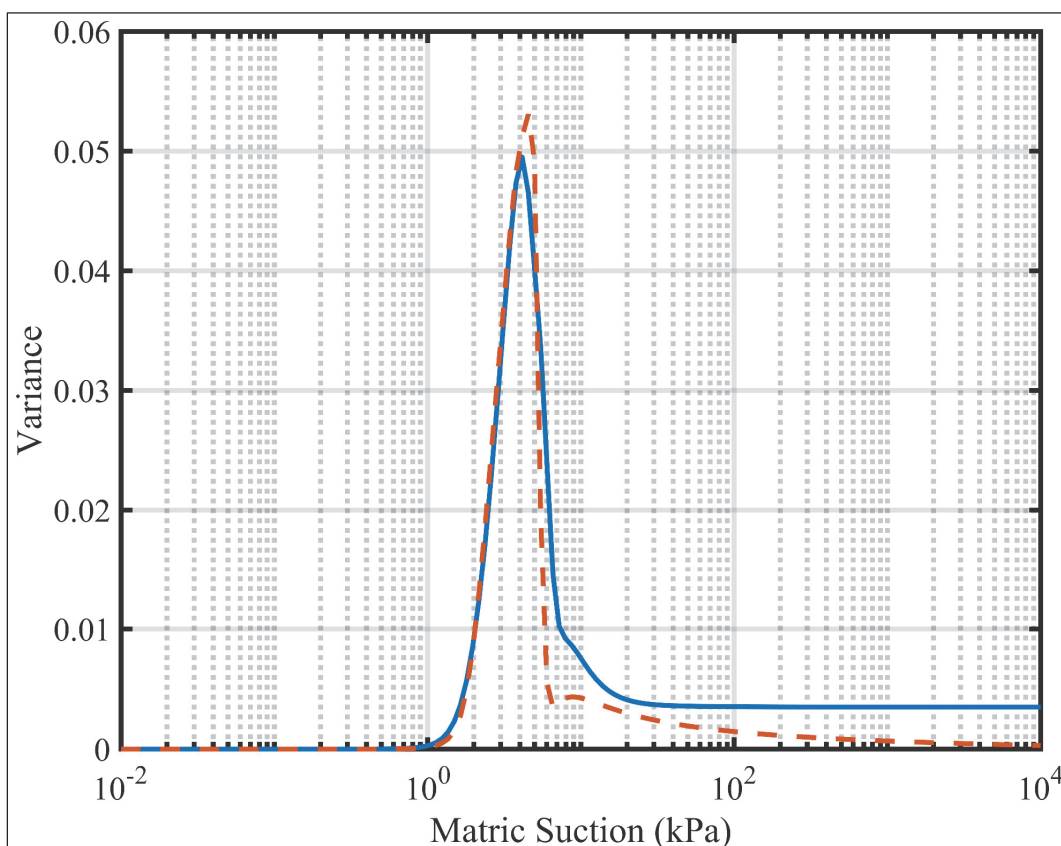


Figure 31. Variance across preparation energies for samples prepared at 30 percent saturation level.



The variance of the samples prepared at a saturation of 24 percent (Figure 30) was the lowest of the three saturations tested, but the variance was still within the same order of magnitude as the other two saturation levels. The lower variance calculated for the samples prepared at 24 percent saturation is likely due to the population of the 24 percent saturation sample sets being larger than those of the other two saturation levels. The reason for the sample sets being so much larger for the 24 percent saturation was that the samples for each of the energy levels were tested in duplicate on the TRIM device. Due to the quantity of time needed to perform SWCC testing with the Fredlund device, duplicates were not attempted. Therefore, the TRIM device results likely skewed the variance calculation.

Within Figures 29, 30, and 31, the variance near the AEV are typically the largest while they drop off significantly following the peak variance value approaching the residual value. For the Fredlund and Xing models, the variance was larger near the AEV. In contrast, the variance was larger near the residual conditions for the van Genuchten model when compared to

the Fredlund and Xing model. This is due, in part, to differences in the two models. The van Genuchten model adopts a constant residual water content following the residual suction, while the Fredlund and Xing model gradually approaches zero at 1e6 kPa. For this reason, the van Genuchten model may be more appropriate when the behavior of interest is near the AEV, whereas the Fredlund and Xing model is more suitable when the behavior of the soil with regard to the SWCC is needed near or post-residual condition. Neither model presents a compelling result to suggest better performance in the development of the “true” SWCC for this material, thus the use of either (or both) would be acceptable representations of this soil.

The scatter of data near the AEV is likely due to differences in the testing apparatus as opposed to sample preparation for reasons previously illustrated. To better quantify these differences, a testing plan with multiple testing apparatuses and samples (prepared in the same manner as this investigation and with a population representative of each SWCC testing device) would be necessary to make the results statistically significant.

Table 9 shows both model-fitting parameters for the maximum, mean, and minimum SWCC values for the poorly graded fine sand tested in this investigation. The saturated and residual values are presented in degree of saturation.

**Table 9. Fitting parameters for maximum, mean, and minimum SWCCs.**

curve	van Genuchten				Fredlund and Xing			
	$S_r$	$S_s$	$\alpha$ (1/kPa)	$n$	$S_s$	$a$ (kPa)	$n$	$m$
max	0.23	1.00	0.16	5.26	1.00	5.09	11.40	0.52
mean	0.13	1.00	0.26	3.29	1.00	3.19	3.62	1.00
min	0.05	1.00	0.42	3.06	1.00	2.50	2.81	1.38

Figures 32 and 33 are a graphical representation of Table 9. The range between the minimum and maximum is largest near the AEV and smallest near the residual suction value. The range corresponds well to the variance values plotted in Figures 29, 30, and 31. The response of the soil between the AEV and the residual value is mainly a result of capillary action of the soil pores (Lu and Likos 2004). The capillary action is related to the size and shape of the soil pores and how connected they are. Larger soil pores

would result in lower AEV due to the inverse relationship between matric suction and pore size, as shown in Equation 11.

$$h = \frac{2\sigma}{r\gamma_w} \quad (11)$$

where  $h$  is the capillary rise,  $\sigma$  is the surface tension,  $r$  is the pore size, and  $\gamma_w$  is the unit weight of water (Baver et al. 1972). As matric suction increases, a continuous column of water will occur with a smaller pore radius. Once the smallest pore radius is reached, a continuous column of water will no longer exist in the soil matrix. When the residual suction is reached, any matric suctions that are larger will result in non-continuous water films – at this point capillary law will no longer dominate.

Figure 32. Maximum, mean, and minimum SWCC values for poorly-graded fine sand fitted with van Genuchten model.

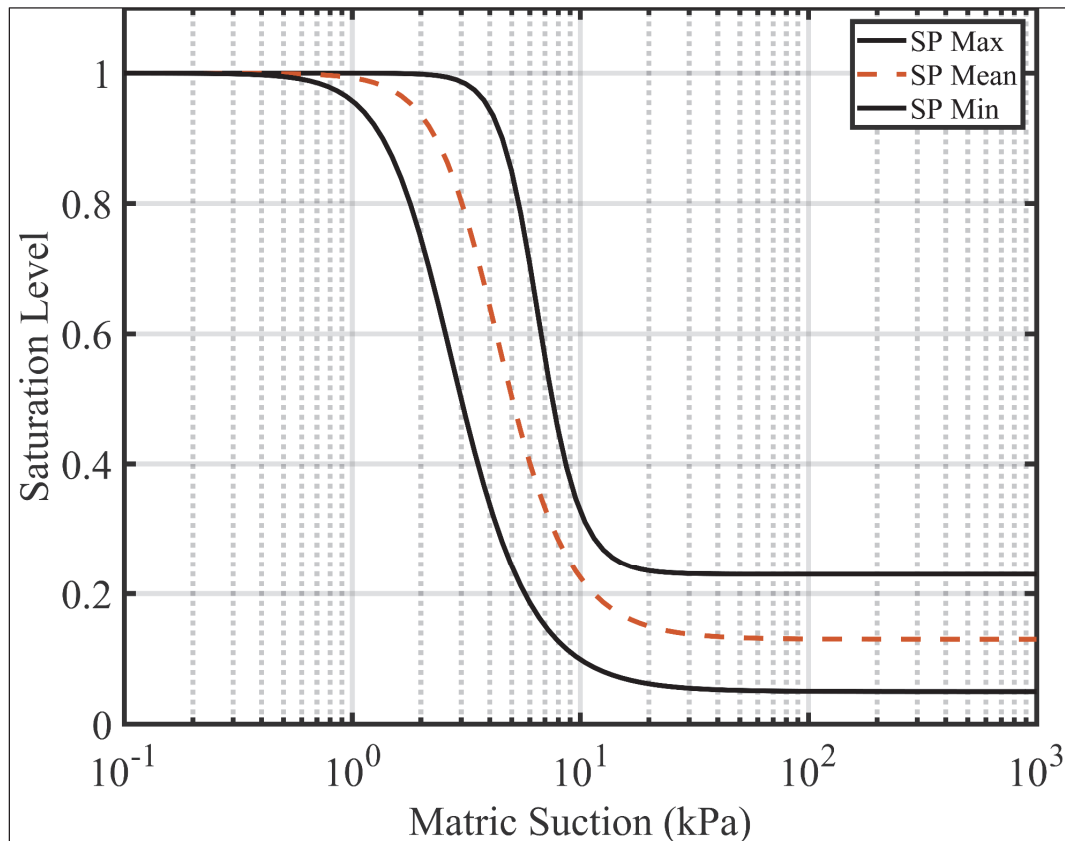
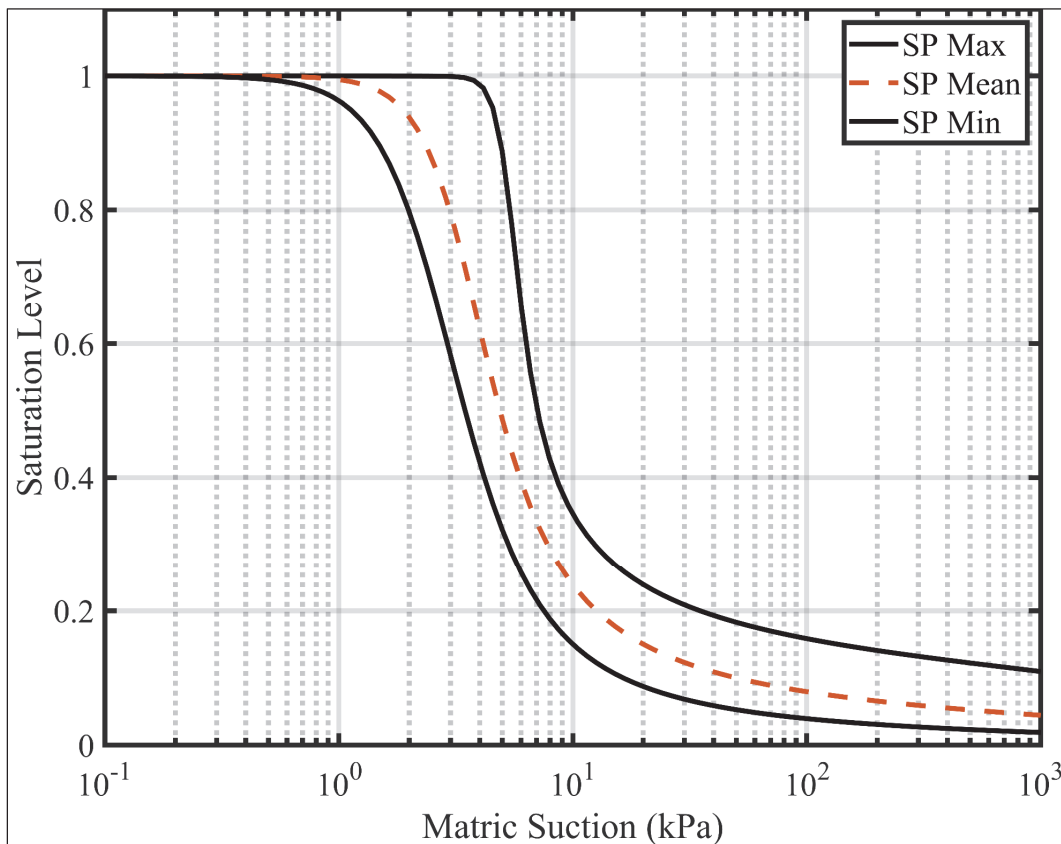


Figure 33. Maximum, mean, and minimum SWCC values for poorly-graded fine sand fitted with Fredlund and Xing model.



The question remains as to whether these curves are representative of sands differing from the sands tested in this investigation. To answer this question, sample SWCC data were attained from the unsaturated soil hydraulic database (UNSODA; Nemes et al. 1999). The samples were selected based on their gradation and textural classification. The textural classification system is the classification system used to categorize agricultural soils based on their grain size. Consistency testing, such as for the Atterburg limits, is not required as part of the textural classification system as it is for the USCS. Table 10 shows the material properties of the samples from the UNSODA database.

Table 10. Soils data for samples selected from UNSODA.

UNSAODA code	$D_{10}$ (mm)	$D_{30}$ (mm)	$D_{60}$ (mm)	$C_u$	$C_c$	USCS*	%passing #200	$k_{sat}$ (cm/s)
1042	0.08	0.15	0.21	2.75	1.30	SP-SM	9.12	7.71E-03
1140	0.06	0.16	0.27	4.18	1.51	SP-SM	11.39	2.05E-03
2310	0.14	0.22	0.36	2.60	0.97	SP	1.45	1.86E-02
3080	0.11	0.15	0.20	1.76	0.97	SP	1.00	2.32E-02
4440	0.14	0.21	0.26	1.87	1.18	SP	4.55	2.22E-03
4441	0.15	0.20	0.24	1.61	1.11	SP	1.95	1.11E-02
4442	0.15	0.22	0.34	2.35	1.00	SP	0.28	5.00E-03
4443	0.21	0.25	0.32	1.56	0.98	SP	0.00	6.00E-03
4661	0.08	0.25	0.42	5.11	1.84	SP-SM	9.30	1.32E-02
1050	0.09	0.31	0.54	5.80	1.93	SP-SM	9.05	8.19E-03
1052	0.08	0.36	0.66	8.22	2.48	SW-SM	9.80	1.29E-02
1053	0.24	0.44	0.73	3.06	1.11	SP-SM	5.19	3.22E-02
1054	0.29	0.50	0.77	2.67	1.13	SP	2.93	4.83E-02
1073	0.17	0.40	0.84	5.03	1.12	SP	4.24	2.41E-02
1074	0.18	0.42	0.83	4.52	1.15	SP	3.40	4.25E-02
1075	0.15	0.37	0.71	4.59	1.25	SP-SM	6.35	3.25E-02
2220	0.03	0.07	0.19	5.86	0.83	SM	32.82	6.99E-04
2221	0.05	0.12	0.29	5.35	0.93	SM	20.33	1.45E-02
4650	0.08	0.25	0.43	5.27	1.83	SP-SM	9.30	1.13E-04
4651	0.10	0.25	0.44	4.48	1.38	SP-SM	6.80	2.20E-03

\*fines classification unknown, silt assumed per USACE ETL-0254 (Wright et al. 1981)

The samples shown in Table 10 are broken into two groups: fine and coarse. These two groups reference the grain size of the sample tested during this investigation. The SWCC fine-grained data from UNSODA was fitted using the van Genuchten and the Fredlund and Xing models as shown in Figures 34 and 35, respectively.

Figure 34. UNSODA fine-grained data set fitted with van Genuchten model.

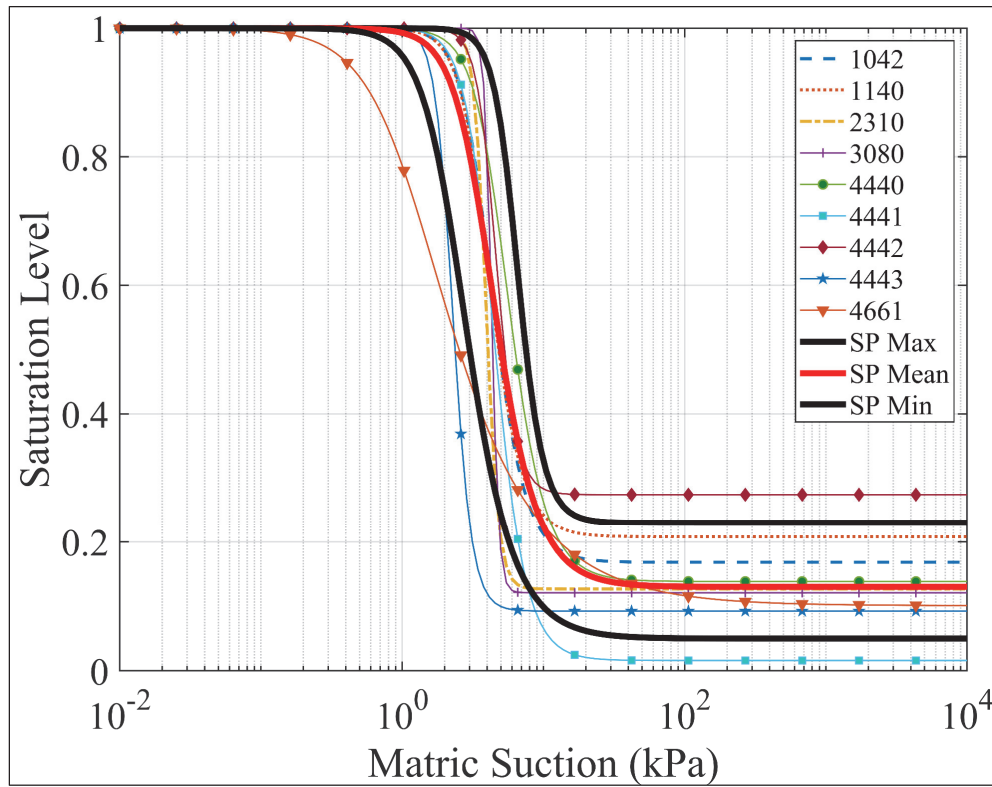
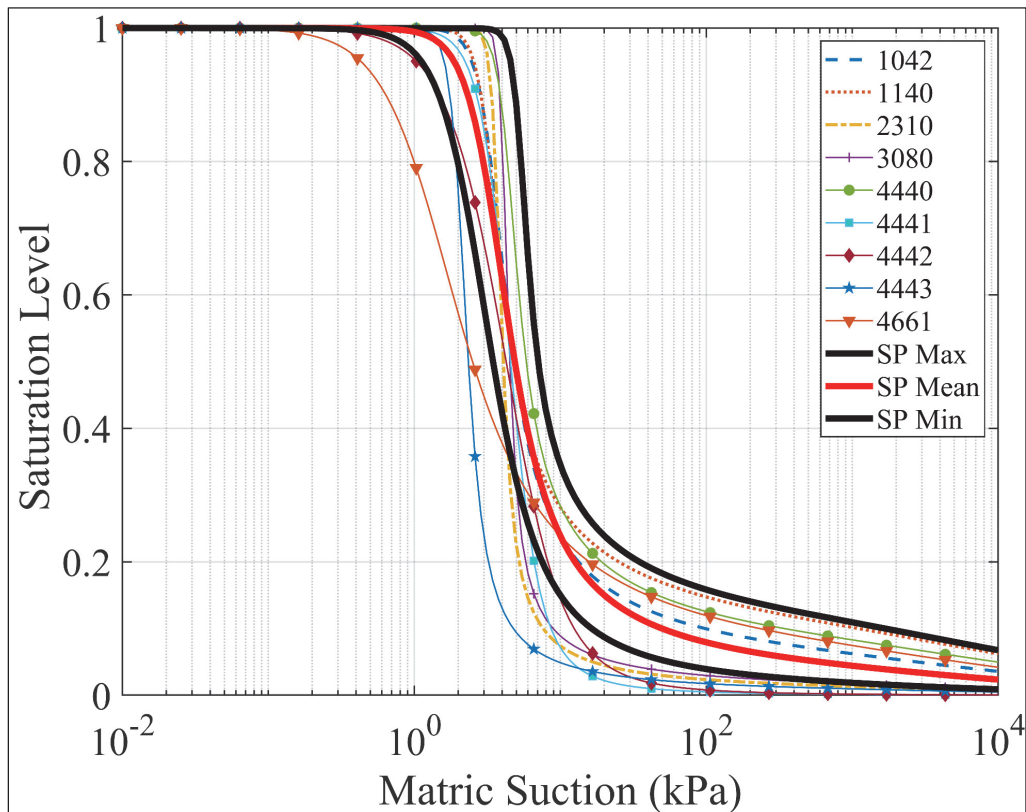
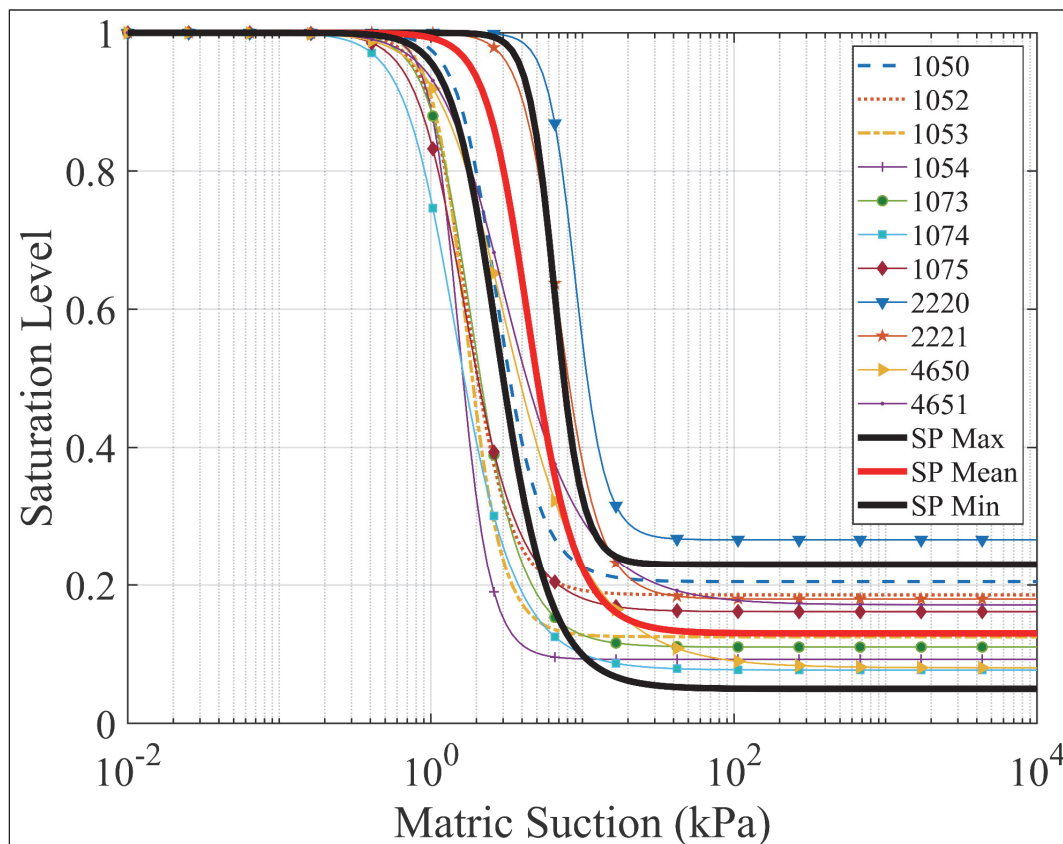


Figure 35. UNSODA fine-grained data set fitted with Fredlund and Xing model.



There are nine samples in the fine group; six of the nine classify as SP according to the USCS. Two of the nine samples, 4443 and 4661, using UNSODA sample codes, fall outside of the confidence intervals defined for the soil tested in the current investigation. Sample 4661 has an AEV much lower than the mean curve but returns within the defined interval near the 35 percent saturation level. Sample 4443 has an AEV near the mean value but deviates from the bounds near the residual value. The sand tested in this investigation, SP-1, was coarser grained than the samples from the fine group, as shown by the grain-size distributions in Figure 36. A majority of the sample SWCCs fall within the bounds defined in this investigation and appear to correspond well to the results of this investigation.

Figure 36. Grain-size distribution of fine group samples.



The SWCC coarse-grained data from UNSODA was fitted by using the same two models. Of the 11 samples contained in the coarse group, eight plot just to the left of the minimum boundary (Figures 37 and 38). This is reasonable considering that these samples are coarser than the samples tested in this investigation. A majority of the samples fall within the bounds following the residual suction value, while the greatest deviation occurs near the AEV. This is expected, considering that because of the

increased grain size of the group, according to capillary law, the soils would de-saturate at lower matric suctions compared to a finer-grained soil. This means that larger pore (grain) sizes would lead to lower AEVs. The only exceptions to this statement are samples 2220 and 2221, which are well-graded, contain considerable fine-grained soil (silt or clay), and classify as SM (or SC). The fines content seems to impact the SWCC in making it correspond to the SWCC of a finer-grained soil even with larger grain sizes present.

Figure 37. UNSODA coarse-grained data set fitted with van Genuchten model.

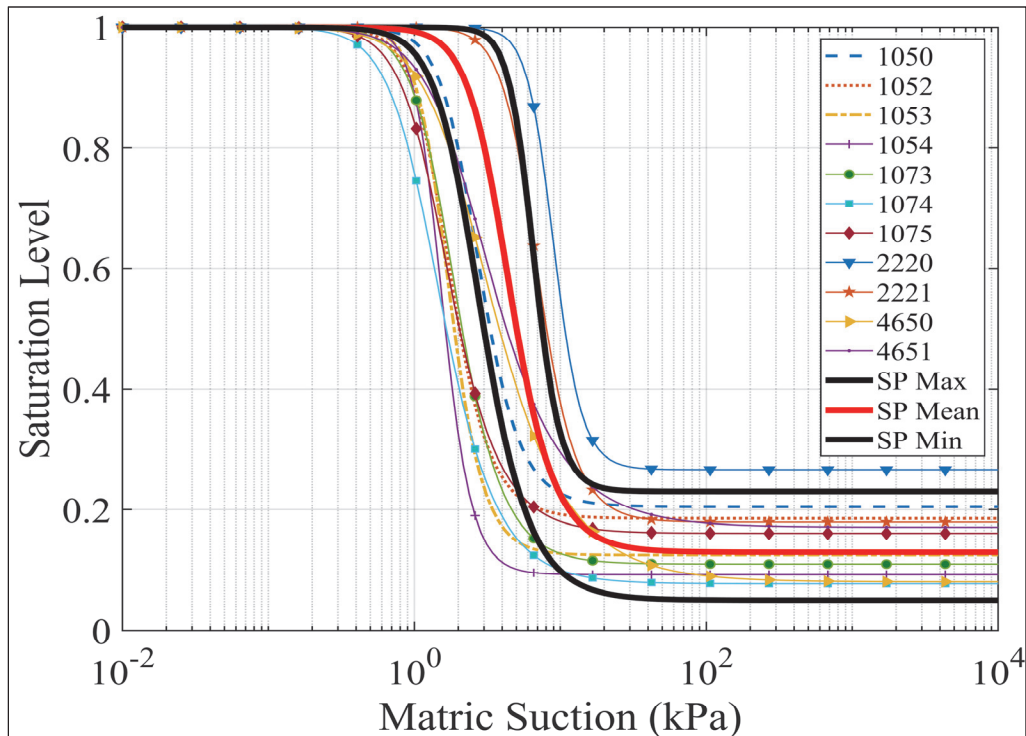
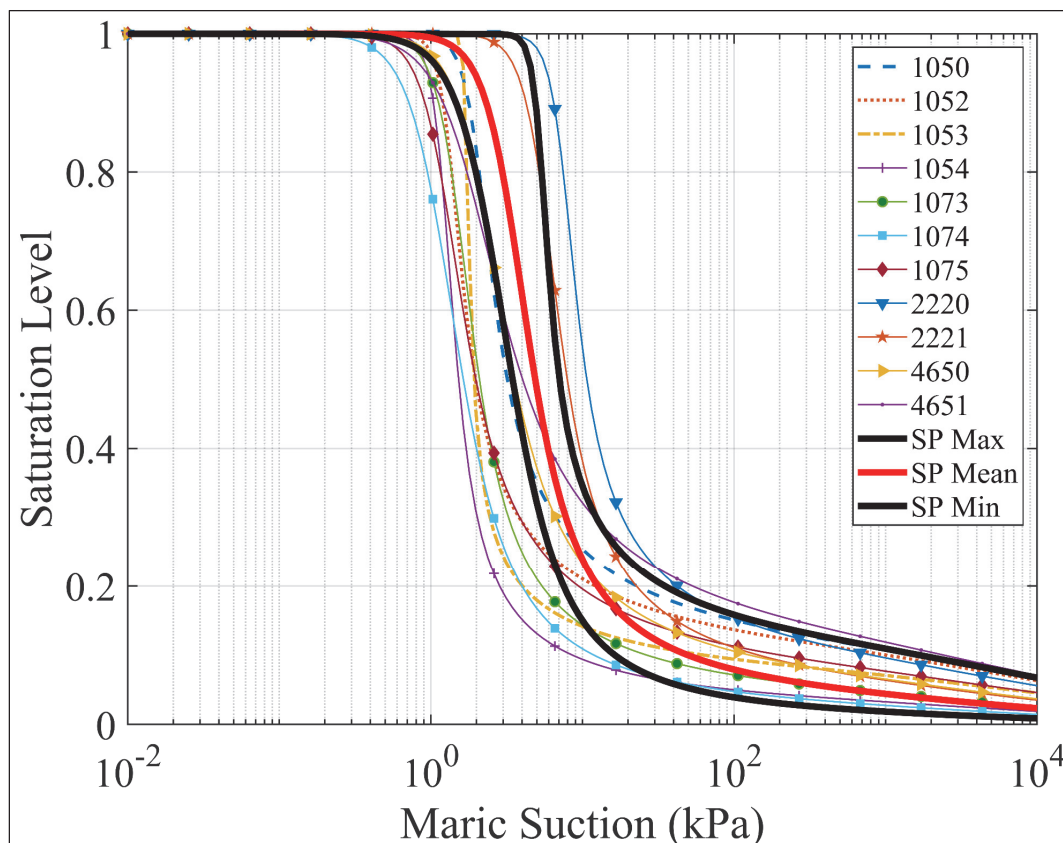


Figure 38. UNSODA coarse-grained data set fitted with Fredlund and Xing model.



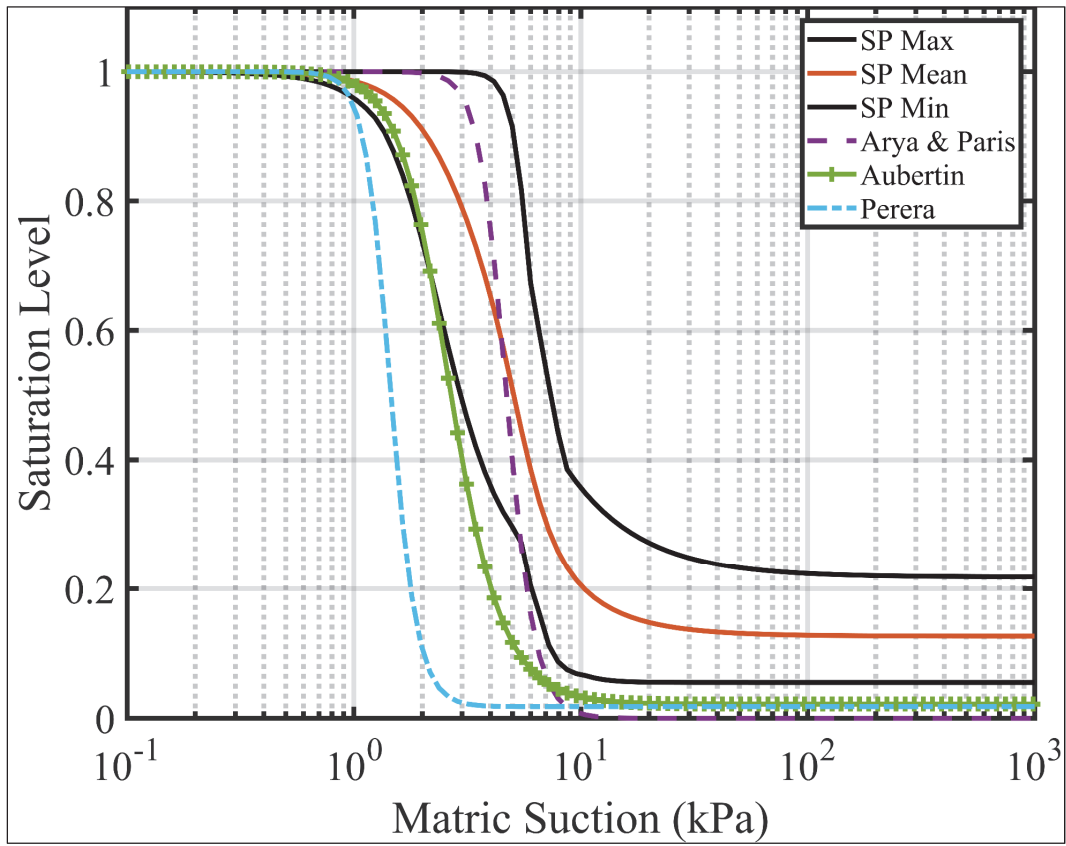
Many methods for predicting SWCC have been developed based on commonly tested material properties (i.e., plasticity, grain size, or hydraulic conductivity). These prediction methods are only as good as the data set from which they were derived. Three predictive methods were employed for comparison to the current testing program: Perera et al. (2005), Aubertin et al. (2003) and Arya and Paris (1981). The Perera method, statistically derived from 154 nonplastic and 63 plastic soils, was developed for plastic and nonplastic soils and uses both the grain size distribution and the plasticity index to predict the Fredlund and Xing parameters. The Aubertin method modified the existing Kovacs model and takes into account both capillary and adhesion forces. The Arya and Paris method was derived from loam, silty clays, and sandy loams and uses the grain size distribution, bulk density, and particle density to predict the SWCC. The parameters derived from each method are shown in Table 11.

Table 11. Fitting parameters for SWCC prediction methods.

Prediction Method	van Genuchten				Fredlund and Xing				
	$\theta_r$	$\theta_s$	$\alpha$ (1/kPa)	$n$	$\theta_s$	$a$ (kPa)	$n$	$m$	$\psi_r$
Arya and Paris	0.00	0.38	0.22	7.30	0.38	8.15	4.22	16.97	1500.00
Aubertin	0.01	0.39	0.42	4.15	0.39	2.11	5.62	1.21	1500.00
Perera	0.01	0.38	0.71	7.79	0.38	1.22	10.76	1.35	100.00

Each of the three prediction methods is plotted along with the minimum, mean, and maximum values from the current investigation, using the van Genuchten model only. All three methods varied considerably with regard to van Genuchten model parameter  $\alpha$  (Figure 39). Both the Aubertin and Perera methods plot near the minimum curve while the Arya and Paris method bisects the mean curve. All of the prediction methods are well below the bounds at matric suction values greater than 7 kPa but provide reasonable approximations at matric suctions less than this value. At matric suction values between AEV and residual value, the Arya and Paris method approximates the results of this investigation.

Figure 39. Prediction methods plotted with the minimum, mean, and maximum values.



## 5 Conclusions

The purpose of this laboratory investigation was to provide representative SWCCs of a fine-grained, poorly graded sand. As part of this investigation, exploring the impact of the testing device and the sample preparation method was conducted by using multiple testing apparatuses and methods as well as preparing samples in a carefully controlled manner that was highly repeatable. Preparing the samples with different compaction energies was done to simulate different soil fabrics that are possible over various depositional environments that may be encountered in the field. The results of this investigation indicated that with regard to a fine-grained poorly graded sand, minimal variation in the SWCC was found. The statistical bounds of the SWCC measured in this investigation, therefore, were found to be representative of the typical SWCC that might be found across a wide range of depositional environments.

The measured SWCC data were fitted by using two common models, and the advantages and limitations of each were shown. The Fredlund and Xing model matches the data well at matric suctions greater than the residual suction and is adequate for matric suctions less than this value. The van Genuchten model diverged from the measured data following the residual suction but matched the data better near the AEV. Therefore, with knowledge of the matric suctions of interest, the more representative model may be chosen.

The measured data set exhibited scatter near the AEV of the fine-grained sand. The scatter of data near the AEV was likely due to differences in the testing apparatus as opposed to sample preparation for reasons previously illustrated. To better quantify these differences, a testing plan with multiple testing apparatuses and samples (prepared in the same manner as this investigation and with a population representative of each SWCC testing device) would be necessary to make the results statistically significant. Future research should be conducted to address this.

The statistical bounds of the SWCC measured in this investigation were compared to a range of SWCCs from a database. The gradation of the SWCCs used in the comparison ranged from fine- to coarse-grained sands and some had appreciable silt and clay. It was found that the coarse-grained soils' SWCCs exhibited the same general shape, but the AEV fell near the minimum bound of the measured SWCC while the fine-grained

samples from the database fell within the measured bounds of the current investigation results. This finding indicated that the results of this investigation are representative of soils with a similar gradation. A further comparison was made between commonly used SWCC prediction methods, and it was found that the method by Arya and Paris approximated the results of this investigation with increased accuracy compared to the other methods investigated. All three methods were approximately within the statistical bounds measured in this investigation, providing further validation of the results of this investigation.

The results of this investigation have been found to be representative of the SWCC for a range of gradations that fall within the USCS-defined fine-grained sand bounds. These results have been compared to other SWCCs of soils with gradations within and just outside these bounds. This comparison indicates that the results are valid for these conditions and are therefore representative for this soil type. The results of this laboratory investigation will be used as the representative SWCC for a fine-grained, poorly graded sand in a soils database. Further testing is required and will be conducted to generate SWCCs representative of other soil types for the same soils database.

## References

- American Society for Testing and Materials (ASTM). 1998. *Standard practice for classification of soils for engineering purposes (Unified Soil Classification System)*. Designation D2487-98. West Conshohocken, PA: ASTM International.
- \_\_\_\_\_. 2010. *Standard test method for measurement of soil potential (suction) using filter paper*. Designation D 5298-10. West Conshohocken, PA: ASTM International.
- \_\_\_\_\_. 2012. *Standard test methods for laboratory compaction characteristics of soil using modified effort (56,000 ft-lbf/ft<sup>3</sup> [2,700 kN-m/m<sup>3</sup>])*. Designation D 1557-12. West Conshohocken, PA: ASTM International.
- Arya, L. M., and J. F. Paris. 1981. A physicoempirical model to predict the soil moisture characteristic from particle-size distribution and bulk density data. *Soil Science Society of America Journal* 45(6):1023-1030.
- Aubertin, M., M. Mbonimpa, B. Bussière, and R. P. Chapuis. 2003. A model to predict the water retention curve from basic geotechnical properties. *Canadian Geotechnical Journal* 40(6):1104-1122.
- Baver, L. D., W. H. Gardner, and W. R. Gardner. 1972. *Soil physics*. 4<sup>th</sup> ed. New York: Wiley.
- Bulut, R., R. L. Lytton, and W. K. Wray. 2001. Soil suction measurements by filter paper. In *Expansive Clay Soils and Vegetative Influence on Shallow Foundations, Proceedings of 2001 Annual Civil Engineering Conference, 10-13 October 2001, Houston, TX*, ed. C. Vipulanandan, M. B. Addison, and M. Hansen, 243-261.
- Fredlund, D. G., and Harianto Rahardjo. 1993. *Soil mechanics for unsaturated soils*. Hoboken, NJ: John Wiley & Sons.
- Fredlund, D. G., H. Rahardjo, and M. D. Fredlund. 2012. *Unsaturated soil mechanics in engineering practice*. Hoboken, NJ: John Wiley & Sons.
- Fredlund, D. G., and A. Xing. 1994. Equations for the soil-water characteristic curve. *Canadian Geotechnical Journal* 31(4):521-532.
- GCTS Testing Systems. n.d. *Fredlund soil water characteristic device operating instruction. Version 1.3*. SWC-150. Tempe, AZ: GCTS.
- Leong, E. C., and H. Rahardjo. 1997. Review of soil-water characteristic curve equations. *Journal of Geotechnical and Geoenvironmental Engineering* 123(12):1106-1117.
- Likos, W. J., N. Lu, and J. W. Godt. 2013. Hysteresis and uncertainty in soil water-retention curve parameters. *Journal of Geotechnical and Geoenvironmental Engineering* 140(4):04013050.
- Lu, N., N. Alsharif, A. Wayllace, and J. W. Godt. 2014. Closing the loop of the soil water retention curve. *Journal of Geotechnical and Geoenvironmental Engineering* 141(1):02814001.

- Lu, N., and W. J. Likos. 2004. *Unsaturated soil mechanics*. Hoboken, NJ: John Wiley & Sons Inc.
- \_\_\_\_\_. 2006. Suction stress characteristic curve for unsaturated soil. *Journal of Geotechnical and Geoenvironmental Engineering* 132(2): 131-142.
- McQueen, I. S., and R. F. Miller. 1974. Approximating soil moisture characteristics from limited data: Empirical evidence and tentative model. *Water Resources Research* 10(3):521-527.
- Mulilis, J. P., H. B. Seed, and C. K. Chan. 1977. Effects of sample preparation on sand liquefaction. *Journal of the Geotechnical Engineering Division* 103(GT2):91-108.
- Nemes, A., M. G. Schaap, and F. J. Leij. 1999. *The UNSODA Unsaturated Soil Hydraulic Database Version 2.0*. Riverside, CA: U.S. Salinity Laboratory.
- Olson, R. E., and L. J. Langfelder. 1965. Pore water pressures in unsaturated soils. *Journal of Soil Mechanics & Foundations Division* 91(4):127-150.
- Perera, Y. Y., C. E. Zapata, W. N. Houston, and S. L. Houston. 2005. Prediction of the soil-water characteristic curve based on grain-size-distribution and index properties. In *Advances in Pavement Engineering, Proceedings of Geo-Frontiers 2005, 24-26 January 2005, Austin, TX*, ed. C. W. Schwartz, E. Tutumluer, and L. Tashman, 1-12.
- Richards, L. A. 1931. Capillary conduction of liquids through porous mediums. *Physics* 1(5):318-333.
- Taylor, O.-D. S., W. W. Berry, K. E. Winters, W. R. Rowland, M. D. Antwine, and A. L. Cunningham. 2017. Protocol for cohesionless sample preparation for physical experimentation. *ASTM Geotechnical Testing Journal* 40(2):284-301. Doi: 10.1520/GTJ20150220.
- Trevena, D. H. 1984. Cavitation and the generation of tension in liquids. *Journal of Physics D: Applied Physics* 17(11):2139.
- Vanapalli, S. K., W. S. Sillers, and M. D. Fredlund. 1998. The meaning and relevance of residual state to unsaturated soils. In *Proceedings of the 51st Canadian Geotechnical Conference, 4-7 October*. Edmonton, Alberta.
- van Genuchten, M. T. 1980. A closed-form equation for predicting the hydraulic conductivity of unsaturated soils. *Soil Science Society of America Journal* 44(5):892-898.
- Wayllace, A., and N. Lu. 2011. A transient water release and imbibitions method for rapidly measuring wetting and drying soil water retention and hydraulic conductivity functions. *ASTM Geotechnical Testing Journal* 35(1):1-15. Doi: 10.1520/GTJ103596.
- Winters, K. E., O.-D. S. Taylor, W. W. Berry, W. R. Rowland, M. D. Antwine, and A. L. Cunningham. 2016. Cohesionless soil fabric and shear strength at low confining pressures. Paper presented at ASCE Geo-Chicago Conference, Chicago, 2016. Doi: 10.1061/9780784480151.022.

Wright, J. S., T. C. Vogel, A. R. Pearson, and J. A. Messmore. 1981. *Terrain analysis procedural guide for soil, February 1981*. ETL-0254. Fort Belvoir, VA: U.S. Army Corps of Engineers.

# REPORT DOCUMENTATION PAGE

Form Approved  
OMB No. 0704-0188

Public reporting burden for this collection of information is estimated to average 1 hour per response, including the time for reviewing instructions, searching existing data sources, gathering and maintaining the data needed, and completing and reviewing this collection of information. Send comments regarding this burden estimate or any other aspect of this collection of information, including suggestions for reducing this burden to Department of Defense, Washington Headquarters Services, Directorate for Information Operations and Reports (0704-0188), 1215 Jefferson Davis Highway, Suite 1204, Arlington, VA 22202-4302. Respondents should be aware that notwithstanding any other provision of law, no person shall be subject to any penalty for failing to comply with a collection of information if it does not display a currently valid OMB control number. **PLEASE DO NOT RETURN YOUR FORM TO THE ABOVE ADDRESS.**

<b>1. REPORT DATE (DD-MM-YYYY)</b> August 2019		<b>2. REPORT TYPE</b> Tech Report		<b>3. DATES COVERED (From - To)</b>	
<b>4. TITLE AND SUBTITLE</b>  Laboratory Measure of SWCC for a Poorly Graded Fine Sand				<b>5a. CONTRACT NUMBER</b>	
				<b>5b. GRANT NUMBER</b>	
				<b>5c. PROGRAM ELEMENT NUMBER</b>	
<b>6. AUTHOR(S)</b> Lucas A. Walshire, Oliver-Denzil S. Taylor, and Woodman W. Berry				<b>5d. PROJECT NUMBER</b> 62784	
				<b>5e. TASK NUMBER</b>	
				<b>5f. WORK UNIT NUMBER</b>	
<b>7. PERFORMING ORGANIZATION NAME(S) AND ADDRESS(ES)</b>  Geotechnical and Structures Laboratory U.S. Army Engineer Research and Development Center 3909 Halls Ferry Road Vicksburg, MS 39180-6199				<b>8. PERFORMING ORGANIZATION REPORT NUMBER</b>  ERDC/GSL TR-19-38	
<b>9. SPONSORING / MONITORING AGENCY NAME(S) AND ADDRESS(ES)</b> U.S. Army Corps of Engineers Washington, DC 20314-1000				<b>10. SPONSOR/MONITOR'S ACRONYM(S)</b>  USACE	
				<b>11. SPONSOR/MONITOR'S REPORT NUMBER(S)</b>	
<b>12. DISTRIBUTION / AVAILABILITY STATEMENT</b> Approved for public release; distribution is unlimited.					
<b>13. SUPPLEMENTARY NOTES</b>					
<b>14. ABSTRACT</b> A laboratory testing program was undertaken to investigate the effects of soil fabrics and densities on the Soil Water Characteristic Curve (SWCC) of a poorly graded (SP), fine-grained sand. The program also better developed the capability to assess soils remotely under both discrete and multivariable geotechnical, geological, and environmental conditions. The results initiate both a soils database to define a baseline behavior and a predictive model for changes in soil characteristics (strength) and behavior (volumetric) under varying meteorological conditions.  The laboratory testing program reconstituted the fine-grained sand samples dry of optimum saturation. An energy-based sample preparation method was then used to build samples comparable to <i>in-situ</i> soil fabrics. Four preparation reconstitution energies and three saturation levels generated soil fabrics within a band of possible densities limited by the soil's mechanical properties. The Transient Release and Imbibition Method (TRIM), the Fredlund device, and the filter paper method (FPM) were used to develop a statistically representative laboratory SWCC over the range of densities and soil fabrics. Testing results indicate that the Fredlund device and TRIM measure the SWCC independently of preparation energy and saturation, as the mean SWCC and the median, maximum, and minimum curves fall within the same range of values.					
<b>15. SUBJECT TERMS</b> Seepage Soil moisture		Soil mechanics Soil physics Sandy soils			
<b>16. SECURITY CLASSIFICATION OF:</b>			<b>17. LIMITATION OF ABSTRACT</b>	<b>18. NUMBER OF PAGES</b>	<b>19a. NAME OF RESPONSIBLE PERSON</b>
<b>a. REPORT</b> UNCLASSIFIED	<b>b. ABSTRACT</b> UNCLASSIFIED	<b>c. THIS PAGE</b> UNCLASSIFIED			69